Water Research 207 (2021) 117812

Contents lists available at ScienceDirect

Water Research

journal homepage: www.elsevier.com/locate/watres

Oxidation of 51 micropollutants during drinking water ozonation: Formation of transformation products and their fate during biological post-filtration

Rebekka Gulde [a], Baptiste Clerc [a], Moreno Rutsch [a], Jakob Helbing [b], Elisabeth Salhi [a], Christa S. McArdell [a], Urs von Gunten [a,c,d,*]

[a] Eawag, Swiss Federal Institute of Aquatic Science and Technology, Dübendorf, CH-8600 Switzerland
[b] Zürich Water Works, Zürich, CH-8021, Switzerland
[c] School of Architecture, Civil and Environmental Engineering (ENAC), Ecole Polytechnique Fédérale de Lausanne (EPFL), Lausanne, CH-1015 Switzerland
[d] Institute of Biogeochemistry and Pollutant Dynamics (IBP), ETH Zurich, Zurich, CH-8092, Switzerland

ARTICLE INFO

Keywords:
Ozone
Hydroxyl radical
Sand filter
Transformation products
Abatement
Lake water

ABSTRACT

Micropollutants (MP) with varying ozone-reactive moieties were spiked to lake water in the influent of a drinking water pilot plant consisting of an ozonation followed by a biological sand filtration. During ozonation, 227 transformation products (OTPs) from 39 of the spiked 51 MPs were detected after solid phase extraction by liquid chromatography high-resolution mass spectrometry (LC-HRMS/MS). Based on the MS/MS data, tentative molecular structures are proposed. Reaction mechanisms for the formation of a large number of OTPs are suggested by combination of the kinetics of formation and abatement and state-of-the-art knowledge on ozone and hydroxyl radical chemistry. OTPs forming as primary or higher generation products from the oxidation of MPs could be differentiated. However, some expected products from the reactions of ozone with activated aromatic compounds and olefins were not detected with the applied analytical procedure. 187 OTPs were present in the sand filtration in sufficiently high concentrations to elucidate their fate in this treatment step. 35 of these OTPs (19%) were abated in the sand filtration step, most likely due to biodegradation. Only 24 (13%) of the OTPs were abated more efficiently than the parent compounds, with a dependency on the functional group of the parent MPs and OTPs. Overall, this study provides evidence, that the common assumption that OTPs are easily abated in biological post-treatment is not generally valid. Nevertheless, it is unknown how the OTPs, which escaped detection, would have behaved in the biological post-treatment.

1. Introduction

Oxidation processes have been applied for water disinfection for more than a century (von Gunten 2018). Since several decades such processes are also applied for the oxidative abatement of micropollutants, with a strong focus on ozonation and advanced oxidation processes (AOPs) (von Gunten 2018). The efficiency of the abatement of micropollutants during oxidation processes depends on reaction kinetics, which is related to the structural features of the target compounds (Lee and von Gunten 2012). Typically, micropollutants are not mineralized and a suite of transformation products is formed (Lee et al., 2015; Lee and von Gunten 2016; von Sonntag and von Gunten 2012). During ozonation and AOPs, the formed transformation products have often only limited residual biological activity related to the originally intended effects (Lee and von Gunten 2016; von Sonntag and von Gunten 2012).

Ozonation processes are currently also applied for enhanced treatment of municipal wastewater treatment plant effluents to protect the aquatic environment or for potable reuse purposes (Eggen et al., 2014; Gerrity et al., 2013; Hollender et al., 2009; Huber et al., 2003; Olivieri et al., 2016; Reungoat et al., 2012; Reungoat et al., 2010; Ternes et al., 2003). Due to the formation of mostly low molecular weight biodegradable organic compounds such as aldehydes, ketones and carboxylic acids (summarized as assimilable organic carbon, AOC; biodegradable organic carbon, BDOC) during ozonation of waters containing dissolved organic matter (DOM), it is generally followed by a biological

* Corresponding author at: Eawag, Swiss Federal Institute of Aquatic Science and Technology, Dübendorf, CH-8600 Switzerland.
E-mail address: vongunten@eawag.ch (U. von Gunten).

https://doi.org/10.1016/j.watres.2021.117812
Received 18 August 2021; Received in revised form 19 October 2021; Accepted 22 October 2021
Available online 28 October 2021

post-treatment to abate AOC/BDOC (Bourgin et al., 2018; Gulde et al., 2021; Hammes et al., 2006; Marron et al., 2020; Rosario-Ortiz et al., 2016; Van der Kooij et al. 1989; von Sonntag and von Gunten 2012; Zimmermann et al., 2011). It has also been demonstrated that toxicity, which can be formed during ozonation (probably related to aldehydes, ketones, etc.), is mostly abated during biological post-filtration (Prasse et al., 2015; Stalter et al., 2010). Based on these observations, it has often been suggested that biological post-treatment will also degrade transformation products (OTPs) formed from micropollutants during ozonation. The fate of OTPs (from the direct reaction with ozone) during biological processes has been theoretically assessed previously (Hübner et al., 2015). It has been concluded in that study, that OTPs from amine-containing compounds with a *N*-oxidation are generally less biodegradable than those formed from aromatic (ring opening products) and olefinic compounds (aldehyde and ketone formation) (von Sonntag and von Gunten 2012). This could be at least partially confirmed in one study on the biodegradability of OTPs of carbamazepine (Hübner et al., 2014). Recently, it has been demonstrated that biological post-treatment after ozonation of municipal wastewater effluents has little effect on the abatement of many different transformation products (Bourgin et al., 2018; Gulde et al., 2021; Kharel et al., 2021). However, two of these studies had a partial bias on amine-type compounds (especially tertiary amines with the ensuing formation of *N*-oxides (von Sonntag and von Gunten 2012)). One additional difference between the theoretical study by Hübner et al. (2015) and ozonation in real water systems, is the role of hydroxyl radicals ($^{\bullet}$OH), which are formed as secondary oxidants from the ozone decomposition (Hoigné and Bader 1975; Staehelin et al., 1984). Since $^{\bullet}$OH are very reactive with organic compounds, a significantly higher number and variety of transformation products can be expected in presence of this oxidant (von Sonntag and Schuchmann 1997).

So far, a systematic evaluation of the formation of OTPs from target compounds with various ozone-reactive functional groups is missing for realistic ozonation conditions. Furthermore, there is only limited experimental information on the fate of micropollutants and the corresponding OTPs in biological post-filtration after ozonation.

The goal of this study was to systematically evaluate the formation of OTPs from a large selection of target compounds by kinetic and mechanistic considerations and compare the abatement of OTPs with their parent micropollutants in a post-treatment by a biological sand filter. Fifty-one micropollutants were selected, most of them with distinct ozone-reactive sites, some with only low ozone-reactivity. The experiments were carried out on a pilot plant for drinking water production, consisting of an ozonation reactor with a post-treatment by biological sand filtration, where the selected micropollutants were spiked to the raw lake water. Water samples taken at 12 different locations throughout the treatment train were measured after solid phase extraction with liquid chromatography coupled to high-resolution mass spectrometry (LC-HRMS/MS). A screening for the formation of transformation product signals from the selected parent micropollutants was performed based on signals that were detected in laboratory ozonation experiments with a synthetic water matrix mimicking realistic conditions. The structures of the OTPs were elucidated and the formation of the OTPs was rationalized by kinetic and mechanistic information on ozone and $^{\bullet}$OH radical chemistry. Furthermore, the fate of the OTPs in the biological sand filtration was compared to the fate of their respective parent compounds, which were spiked directly on the sand filter.

2. Material and methods

2.1. Micropollutant selection and preparation of stock solution

Fifty-one micropollutants (MPs) were selected based on the presence of ozone-reactive functional groups, whereby preferably only one such functional group was present in the structure, and based on their abundance in wastewater effluents. The structures of the selected MPs are provided in the Supporting Information 2 (SI2):

Nine tertiary (3°) amines: cetirizine (CET), citalopram (CIT), clarithromycin (CLA), diphenhydramine (DIP), fenpropidin (FEN), lidocaine (LID), sulpiride (SUL), tramadol (TRA), venlafaxine (VEN).

Three secondary (2°) amines: atenolol (ATE), flecainide (FLE), metoprolol (MTO).

Two primary (1°) amines: gabapentin (GAB), sitagliptin (SIT)

Five olefins, one ethyne: carbamazepine (CBZ), caffeine (COF), methylprednisolone (MPN), phenazone (PHE), propyzamide (PYZ).

Eleven (activated) aromatic compounds: 2,4-dichlorophenoxyacetic acid (24D), benzophenone-3 (BZP), benzotriazole (BZT), bezafibrate (BZF), diclofenac (DIC), hydrochlorothiazide (HCT), mecoprop (MEC), naproxen (NAP), sulfamethoxazole (SMX), sulfamethazine (SMZ), trimethoprim (TRI).

Two sulfur-containing compounds: benzisothiazolone (BIT), emtricitabine (EMT).

Seven micropollutants contained two ozone-reactive functional groups: cephalexin (CPX, olefin and thioether), clindamycin (CLI, 3°amine and thioether), mycophenolic acid (MYA, olefin and activated aromatic moiety), oseltamivir (OSE, olefin and 1°amine), propranolol (PRO, 2°amine and activated aromatic moiety), ranitidine (RAN, 3°amine and thioether), resveratrol (RES, olefin and activated aromatic moiety).

Twelve micropollutants contained functional groups with low ozone reactivity (predominant reaction with $^{\bullet}$OH radicals): acesulfame (ACE), atrazine (ATZ), diuron (DIU), ibuprofen (IBU), ketoprofen (KET), lamotrigine (LAM), metformin (MET), oxcarbazepine (OXC), prometon (PRM), sucralose (SUC), thiacloprid (THI), valsartan (VAL).

The selected micropollutants are mainly pharmaceuticals (36), pesticides and/or biocides (9). Among the others were food additives, a corrosion inhibitor, a personal care product, a dietary supplement, and a stimulant (see SI5).

A stock solution of all 51 MPs was prepared (30 mg/L each, in 10 L deionized water). To guarantee a complete dissolution, the solution was stirred at 40 °C overnight and subsequently filtered through a glass microfiber filter (GF/D, 2.7 μm pore size, Whatman). The stock solution was then diluted with tap water to a total volume of 120 L resulting in a MP concentration of 2.5 mg/L each, before dosing to the raw water of the pilot plant. See Section 2.3 for MP dosing in laboratory experiments.

2.2. Pilot-scale ozonation with post-treatment by biological sand filtration

Ozonation experiments were performed with a pilot-scale reactor followed by a biological sand filtration as described in more detail previously (Bourgin et al., 2017) (Fig. S1, SI3). Ultra-filtrated Lake Zürich water was continuously fed into a 4 chamber reactor with a total volume of 2.2 m^3 (Kaiser et al., 2013) operated at a flow of 4.2 m^3/h. Continuous spiking of the MP mixture (2.5 mg/L) to the raw water (final concentration of ≈ 1 μg/L for each MP) was started 17 h before sampling, to enable steady-state conditions (about 2.5 times the hydraulic residence time of the whole system).

After spiking the MPs to the main flow, ozone (produced from oxygen gas by an ozone generator (Ozonia, Switzerland)) was injected to a side stream (10% of the water flow) and passed through a static mixer. After mixing the ozone-enriched side stream into the main stream and passing through a second static mixer, a transferred ozone dose of 1 mg/L (0.8 gO_3/gDOC) was achieved. The ozone reactor had 6 sampling points: before ozone addition (O3in), right after mixing the ozone-enriched side stream to the main stream (O3SP0), 3 sampling points in the ozone reactor (O3SP1, O3SP2, O3SP3) at hydraulic residence times of about 8.3, 16.5, and 24.8 min, respectively, and at the outlet of the reactor (O3out, 33 min) (Fig. S1 and Table S1, SI3). Approximately a quarter of the water flow (0.95 m^3/h) was fed into a cylindric sand filter (height 2 m, area 0.95 m^2, bed volume 1.9 m^3, residence time 2 h). 2.61 × 10^3 kg washed sand skimmed from a slow sand filter of the full-scale drinking water plant Lengg, Zurich (Switzerland) was transferred to the sand filter column. Ozonated ultra-filtrated Lake Zürich water without

MP spiking was fed to the sand filter for 12 months prior to the ozonation experiments to enable growth of a stable microbial community. The biological activity was tested before the ozonation experiments by spiking and measuring the abatement of paracetamol, atenolol, valsartan and carbamazepine, which are known to be bio-transformed to different extents in activated sludge of wastewater treatment plants (Helbling et al., 2012) (Fig. S2, SI3). Five sampling points were selected at the cylindric sand filter at depths of 20, 40, 80, 120, and 160 cm (SF20, SF40, SF80, SF120, SF160) and one at the outlet (SFout) (Fig. S1, SI3). Replicate samples were taken at three different time points (17, 19.5, and 22.5 h after the start of MP spiking) in reverse direction, *i.e.*, from SFout to O3in. The sampling tap was opened for approximately 1 min before water samples were taken. At each sampling point, two water samples were taken. First, for the analysis of OTPs via LC-HRMS/MS, 100 mL water was added to a 100 mL Schott bottle that was spiked with 500 µL of a fresh Na_2SO_3 solution (50 mM) immediately before sampling to quench ozone. These samples were kept at 4 °C in the dark until analysis. Second, the residual ozone concentration was determined by the indigo method (Bader and Hoigne 1981). The pH, DOC concentration and temperature during the experimental campaign were stable at 7.8, 1.2 mg/L and 6 °C, respectively.

To compare the fate of the OTPs with the corresponding parent MPs in sand filtration, the experiment was repeated without ozone dosing. After the last sampling of the above described experiment, the addition of ozone was stopped, while the spiking of the MPs was continued. To ensure steady state conditions, sampling was conducted 15, 17.5 and 20.5 h after stopping the ozonation. Sampling was performed similarly at the sampling points SFout, SF160, SF120, SF80, SF40, SF20, SFin=O3out for the analysis of MPs by LC-HRMS/MS. Additionally, sand samples were taken after the last water sampling at a depth of 175, 140, 105, 70, 35, 20, and 10 cm in triplicates to measure the bacterial abundance via the protein content (Fig. S3, SI3) by a slightly adapted method from Rudolf von Rohr et al. (2014) (Text S1, SI3).

2.3. Ozonation batch experiments (O3bAll)

A laboratory ozonation batch experiment was conducted in a matrix constituted of a similar ozone and $^{\bullet}OH$ exposure as the lake water but only with surrogate organic matter (methanol and acetate) to enable OTP peak verification. In this ozonation batch experiment (*O3bAll*) all parent MPs were spiked together to final concentrations of 1 µg/L, while methanol and acetate were added as promoters and inhibitors, respectively, to simulate the ozone decay and $^{\bullet}OH$ radical formation (Elovitz and von Gunten 1999). Details for these experiments are provided in Gulde et al., (2021). Briefly, 1.3 mg/L ozone was added to the experimental solution at room temperature containing methanol (0.029 mM) and acetate (0.15 mM) in a phosphate buffer adjusted to pH 7.5, which corresponds to a $^{\bullet}OH$ scavenging rate of a DOC concentration of 1.3 mg/L. Aliquots were taken over the course of the experiments (before, and 53, 158, 308, 488 s after ozone addition), quenched with sulfite and kept at 4 °C in the dark until LC-HRMS/MS analysis. Additional experiments performed earlier allowed the backtracking of the parent MP to each of the formed OTP (see Gulde et al. (2021)).

2.4. Chemical analysis and evaluation of results

2.4.1. Determination of ozone and $^{\bullet}OH$-radical exposures in the pilot-plant samples

Ozone exposure ($\int[O_3]dt$) could be determined from the area under the measured ozone depletion curves (from ozone concentrations at sampling points, Figs. S1 and S4, and Table S1, SI3), as the ozone reactor in the pilot-plant was previously assessed to be close to a plug-flow reactor (Gresch et al., 2009; Kaiser et al., 2013; von Gunten and Hoigné 1994). The R_{ct} (ratio of the concentrations of $^{\bullet}OH$:O_3 (Elovitz and von Gunten 1999)) was calculated from the abatement of the ozone-resistant compounds, atrazine, ibuprofen and ketoprofen according to previous studies (Bourgin et al., 2017; Elovitz and von Gunten 1999).

2.4.2. LC-HRMS/MS method for analysis of micropollutants and their OTPs

For the MP and OTP analyses an online solid phase extraction (SPE) coupled to a LC-HRMS/MS measurement was applied. Details on the method, including the used internal standard solutions, are provided in Gulde et al. (2021). Samples from the pilot plant were centrifuged (10 min, 4300 rpm) and 19.5 mL were mixed with 0.5 mL ultra-purified water (Barnstead NanoPure, Thermo Scientific, Switzerland) containing 16 µL internal standard solution (250 mg/L for a final amount of 4 ng on the column). For the preparation of the *O3bAll* samples, 5 mL of the sulfite quenched sample were mixed with 15 mL ultra-purified water containing 16 µL internal standard solution. The prepared 20 mL samples were loaded on SPE cartridges (9 mg Oasis HLB and 9 mg of a mixture of Strata-X-AW/Strata-X-CW/ENV 1/1/1.5), which were eluted with methanol containing 0.1% formic acid. The chromatographic separation was carried out with an C18 Atlantis T3 column (particle size 5 µm, 3.0 × 150 mm, Waters) using a gradient of ultra-purified water and methanol both acidified with 0.1% formic acid as eluents. HR-MS and MS/MS acquisition were obtained by a Q Exactive MS instrument (Thermo Scientific) with $R = 140{,}000$ (at m/z 200) and data-dependent MS/MS ($R = 17{,}500$, Top 7, dynamic exclusion 5 s). Data-dependent MS^2 were triggered at OTP masses that were identified from a previous study (Gulde et al., 2021). Separate runs for positive and negative electrospray ionization mode were acquired.

2.4.3. Identification of OTP signals forming in the pilot plant experiment

To identify OTP signals, the software Compound Discoverer 2.1 (Thermo Scientific) was used separately for positive and negative mode acquisitions. All data from the pilot plant experiment were processed together with the data from the *O3bAll* experiment. To identify OTP signals that form in both the pilot-scale ozonation experiment and in the *O3bAll* experiment, an automatic filter and a manual selection was used. The automatic filter had the following criteria: Signals had to (i) be detectable at least at one sampling point in all three replicates from the pilot plant experiments, (ii) be at least 5 times higher than in the raw water before spiking of the MPs (blind), (iii) be detectable in at least one sampling point of the *O3bAll* experiment, (iv) increase in the *O3bAll* experiment at least two times from the reference sample before ozone addition to a later time point, (v) have a retention time between 4 and 28 min; and (vi) have an area of at least 100′000 or 50′000 in positive or negative mode, respectively. Additionally, signals were manually selected based on (i) reasonable presence (clearly distinguishable from noise) in the samples of the pilot plant and the laboratory ozonation experiments and absence in blind samples, (ii) presence on the list of previously identified OTP signals for each MP determined in an earlier study (Gulde et al. (2021), O3bMix), and (iii) a reasonable peak shape. The assignment of parent MPs was possible thanks to the earlier experiments (*O3bMix* samples).

2.4.4. Structure elucidation of identified OTPs

The structure elucidation was performed according to a previous study (Gulde et al., 2021), and is only explained here in brief. Since an OTP can form multiple components (different adducts, in-source fragments), related signals were grouped manually based on their RT and peak shapes within Compound Discoverer 2.1. Assumed adducts ($[m+H]^+$, $[m-H]^-$, $[m+FA-H]^-$) and chemical formula were assigned using Xcalibur QualBrowser 4.1 (Thermo Scientific). Plausible OTP structures were proposed based on the information of MS^2 spectra and on known ozone reaction pathways using Compound Discoverer 2.1 and manual interpretation. Confidence levels were assigned as proposed by Schymanski et al., (2014).

2.4.5. Evaluation of the abatement of parent MPs and OTPs

The observed abatement of MPs and OTPs in the ozonation reactor was assessed by the general rate law, which includes the reactions with ozone and •OH (Eq. (1)):

$$\ln\frac{[c]_{t2}}{[c]_{t1}} = -k_{O3}\int_{t_1}^{t_2}[O_3]dt - k_{OH}\int_{t_1}^{t_2}[^{\bullet}OH]dt \quad (1)$$

Where $[c]$ is the concentration of a target compound at times t_1 or t_2, respectively, during ozonation. k_{O3} and k_{OH} are the apparent second-order rate constants for the reactions of the target compound with ozone and •OH, respectively, for the conditions of the experiment (pH 7.8). The previously reported second-order rate constants k_{O3} and k_{OH} are provided in SI5.

To estimate the observed relative abatement or formation of the MPs or the OTPs during sand filtration, the relative change of the concentration (corrected with internal standards) or area (as given by Compound Discoverer), respectively, from the inlet to the outlet of the sand filter was calculated by Eq. (2):

$$c_r = \frac{\widetilde{c}(\text{out}) - \widetilde{c}(\text{in})}{\widetilde{c}(\text{in})} \quad (2)$$

where c_r is the relative change; $\widetilde{c}$ is the mean concentration of parent MPs or peak area of OTPs from the replicates; "out" indicates the sampling point at the outlet of the sand filter, which was SFout if all three replicate values were available (Fig. S1, SI3). If this was not the case, the values of SFout and SF160 were combined. For five OTPs that were already abated at these sampling points, points closer to the inlet were chosen (see SI1). "in" indicates the sampling point at the inlet of the sand filter, which was SF20 if all three replicate values were available, otherwise the values of SF20 and SF40 were combined. Theoretically, it would be better to use the sampling point after the ozonation reactor as "in", however, ozone was still present at this sampling point. Residual ozone was degraded at the top layer of the sand filter with a concurrent formation of •OH as indicated by the sudden decrease and/or increase of some OTPs.

To classify the fate of MPs and OTPs during sand filtration, the following limits were chosen for the relative change (c_r): abatement if $c_r < -20\%$, no abatement or formation if $20\% > c_r \geq -20\%$, and formation if $c_r \geq 20\%$. However, replicate values can scatter substantially and interpretation of only the mean values might lead to meaningless results. Therefore, to identify relevant abatement or formation, the uncertainty of c_r was also taken into account by a Monte Carlo simulation (10,000 samples, lognormal distribution, empirical mean and standard deviation from the replicates). Therewith, the probability of the relative change c_r to be negative ($c_r < 0$) was calculated. An abatement was defined as *relevant abatement* if this probability was $\geq 95\%$ and a formation was defined as *relevant formation* if the probability was $\leq 5\%$. All other combinations (i.e., not relevant abatement, not relevant formation, not relevant and no abatement or formation, and relevant and no abatement or formation) were defined as *stable*.

To estimate if an OTP was better abated than its respective parent MP, the difference of the relative change was calculated by Eq. (3):

$$\Delta c_r = c_{r,OTP} - c_{r,MP} \quad (3)$$

Also, here a Monte Carlo simulation (10,000 samples, lognormal distribution, empirical mean and standard deviation from the replicates) was used to point out meaningful results by calculating the probability of ($\Delta c_r < 0$). The abatement capacity of an OTP in comparison to its respective parent MP was treated as *better* if this value was $\geq 90\%$, as *similar* if this value was between 10% and 90%, and as *worse* if this value was $\leq 10\%$.

2.4.6. Bromate formation

Samples were taken before, during and after ozonation and quenched with indigo for bromide (adapted from Salhi and von Gunten (1999)) and bromate analysis (adapted from Shah et al. (2015)) in the ozone reactor and sand filter. The limits of quantification for bromide and bromate were 10 μg/L and 0.2 μg/L, respectively, with standard deviations of 5–10%.

3. Results and discussion

3.1. Pilot-scale ozonation reactor

3.1.1. Ozonation conditions

Ozonation in the pilot-scale system was performed to elucidate the formation of OTPs from the selected MPs by interpretation of LC-HRMS/MS data of pilot- and batch-samples and kinetic and mechanistic information. The ozonation conditions in the laboratory batch experiments with surrogate organic matter (*O3bAll*) were similar in terms of the general oxidation conditions (specific ozone dose, ozone and •OH exposure and R_{ct} (Fig. S5, SI3)) as in the pilot-scale ozonation reactor. R_{ct} obtained in the ozonation laboratory batch experiments *O3bAll* was $1.45 \pm 0.19 \times 10^{-8}$ (bottom of Fig. S5, SI3) and in the pilot-experiments in the range of $0.5 - 1.0 \times 10^{-8}$ (top of Fig. S5, SI3). These values were similar to seven surface waters in a previous study ($0.12–5.8 \times 10^{-8}$ (Elovitz et al., 2000)). Therefore, in the laboratory system of the current study realistic ozonation conditions were achieved.

3.1.2. Parent MP abatement and OTP formation: study design and overview

Fifty-one MPs were spiked to the raw lake water before ozonation. Ozonation resulted in their abatement and formation of 480 OTP signals, which could be reduced to 274 OTPs after grouping of multiple signals (adducts, in-source fragments). 227 of these OTPs could be unambiguously related to a parent MP thanks to batch experiments performed earlier (Gulde et al., 2021). For all these OTPs a structure elucidation was performed and the corresponding data is shown in SI1. A summary of this data is also provided in SI4 and Table S3 (SI3, only the 187 OTPs with sufficiently high concentrations in the sand filter). The 227 OTPs can be assigned to 39 parent MPs, as no OTPs could be identified for 12 parent OTPs (acesulfame, benzophenone-3, benzotriazole, 2,4-dichlorophenoxyacetic acid, emtricitabine, ketoprofen, metformin, metoprolol, mycophenolic acid, naproxen, ranitidine, resveratrol). The reason for not identifying certain OTPs can be manifold such as the limited analytical window, low concentrations, low stabilities of OTPs, low pre-concentration efficiency, etc. The evolution of all spiked MPs and the corresponding OTPs was analyzed as a function of the ozone exposure and is presented in SI1. Based on this, (tentative) reaction mechanisms for the OTP formation are proposed as presented in SI2 and for selected examples in Figs. 1–5 below.

In the panels presented in SI1 for each OTP, the top two figures show the formation of an OTP in the laboratory experiment (left) and the abatement of the parent MP with the ensuing formation of the OTP as a function of the ozone exposure (see Fig. S1 and Table S1, SI3 for the numerical values) in the three pilot plant experiments (right). In SI1, the compounds are ordered alphabetically with the abbreviation of the parent compound (provided in Section 2.1) and the mode of detection (n: negative, p: positive), the exact mass with four decimal points and the retention time in min. For better reading, OTPs are referred to only by the abbreviation of the parent and the exact mass (without decimal points) in the following text, if they can be unambiguously assigned. Otherwise, also the retention time is provided.

3.1.3. Parent micropollutant abatement and OTP formation: kinetic assessment

The kinetics of the abatement of MPs is a crucial parameter to assess the efficiency of an ozonation and if the primary reaction occurs via ozone and/or •OH attack (Eq. (1)). Due to the generally low •OH exposure during ozonation, only ozone-reactive compounds show high

abatement kinetics. Furthermore, the rate of the formation of OTPs provides information about the transformation efficiency and whether the OTPs are primary, secondary or higher-level transformation products. This information is important for mechanistic considerations to assess to which extent a transformation occurs directly or over several reaction steps and by reactions with ozone or •OH or a combination thereof. These aspects are crucial for the discussion of the product formation in Section 3.1.4.

To get a first impression about the agreement of the observed abatement kinetics of the parent MPs to kinetic data from literature, the % abatement of the target MPs at the sampling point O3SP2 (with an ozone exposure of 14×10^{-3} Ms) was compared to the logarithm of the apparent second-order rate constants for the reactions of the parent compounds with ozone (k_{O3}). As Fig. S6 (SI3) indicates, the expected trends for the MP abatement are generally in good agreement with the results from the pilot-scale experiments.

To assess the MP abatement and OTP formation systematically, a kinetic classification of four different patterns was carried out. This was done by visual inspection of the data, which allowed to distinguish four major trends for the MP abatement and the formation of the first detected OTPs: (i) High abatement kinetics of the MP with a fast increase of the OTP, which is either stable or further abated, (ii) high abatement kinetics of the MP with a slow and steady increase of the OTP, (iii) intermediate abatement kinetics of the MP with a parallel increase of the OTP, and (iv) low abatement kinetics of the MP with a parallel increase of the OTPs.

To illustrate this approach, in the following, some examples are discussed for each trend class. More details are provided in Section 3.1.4, where the formation mechanism for OTPs will be discussed.

(i) High abatement kinetics of the MP (non-detect or very low detect at O_3 exposures = 8×10^{-3} Ms) with fast increase of the OTP, which is either stable or further abated

This is a typical case of a fast reaction of MPs with ozone (with calculated high second-order rate constants ($k > \sim 500$ $M^{-1}s^{-1}$ at 6 °C during pilot-scale ozonation), resulting from a 99% abatement of a MP at an O_3 exposure $= 8 \times 10^{-3}$ Ms). This directly leads to a first generation of transformation products which are ozone-resistant or (slowly) further abated by ozone and •OH. Typically, after the first attack of ozone, many compounds containing only one ozone-reactive functional group have a lower reactivity with ozone (von Sonntag and von Gunten 2012). One case in point is the oxidation of atenolol (ATE, SI1) which reacts with an apparent second-order rate constant of $k_{O3} = 10^4$ $M^{-1}s^{-1}$ at pH 7.8 (20 °C) (Benner et al., 2008) at the secondary amine moiety to form the nitro compound (ATE255) (see SI2), which can further react at the aromatic ring with $k_{O3} = 110$ $M^{-1}s^{-1}$ at 20 °C (Benner et al., 2008). If an activation energy of 55 kJ/mol, as for formate with a similar second-order rate constant $k_{O3} = 46$ $M^{-1}s^{-1}$ at 20 °C (Reisz et al., 2014), is assumed, a k_{O3} of 35 $M^{-1}s^{-1}$ at 6 °C can be calculated for the aromatic ring in ATE by the Arrhenius equation (von Sonntag and von Gunten 2012). This would lead to a calculated 43% abatement of ATE255 for an ozone exposure of 16×10^{-3} Ms. This is very close to the observed ca. 50% further abatement of ATE255 during ozonation from O3SP1 (ozone exposure $= 8 \times 10^{-3}$ Ms) until O3out (ozone exposure $= 24 \times 10^{-3}$ Ms). Therefore, it can be hypothesized that most of the further OTP transformation occurs by a direct ozone reaction. Nevertheless, •OH also plays a certain role (5–10%), however, as shown for atrazine or ibuprofen (SI1 and Fig. S5, SI3), an abatement by this route is not very efficient beyond an ozone exposure of about 8×10^{-3} Ms. During ozonation in laboratory and pilot experiments a short primary phase with high •OH yield by direct electron transfer from DOM to ozone is followed by a secondary phase during which •OH formation occurs more slowly by the ozone decomposition chain reaction (Buffle et al., 2006a; Buffle et al., 2006b; Buffle and von Gunten 2006). For several MPs a similar pattern with a fast abatement of MPs and the formation and relatively fast abatement of the OTPs by predominantly O_3 and partially •OH were found: cephalexin (CPX), flecainide (FLE), oseltamivir (OSE), propranolol (PRO), trimethoprim (TRI).

Another example of a fast and direct formation of a transformation product is the oxidation of carbamazepine (CBZ, SI1) by ozone-attack at the olefin group, which leads to BQM (CBZ251), a previously detected product (Hübner et al., 2014; McDowell et al., 2005). However, its further transformation by direct ozone reaction is slow ($k_{O3} \approx 3$ $M^{-1}s^{-1}$, (McDowell et al., 2005)), which would lead to an abatement of 10% until O3out, based on the measured ozone exposure. However, since an 80% abatement occurs in the pilot experiment, this has to be due to •OH reactions, for which an overall second-order rate constant $k_{OH} = 7 \times 10^9$ $M^{-1}s^{-1}$ was estimated (McDowell et al., 2005). From the abatement of atrazine, an •OH exposure of 1.2×10^{-10} Ms can be calculated by considering both $k_{O3} = 6$ $M^{-1}s^{-1}$ and $k_{OH} = 3 \times 10^9$ $M^{-1}s^{-1}$ (Acero et al., 2000) taking into consideration Eq. (1) and the measured ozone exposure. Combining the O_3 and •OH exposure for CBZ251, an abatement of ca. 65% can be calculated until O3out (ca. 10% by direct ozone reaction, ca. 55% by •OH reaction), which is relatively close to the observed approximatively 80% abatement in the experiment considering the uncertainties of such estimates. Similar trends with an initial dominant reaction of the MPs with ozone, followed by an abatement of the OTPs mostly by •OH are also observed for: cetirizine (CET), clarithromycin (CLA), citalopram (CIT), clindamycin (CLI), Diclophenac (DIC), diphenhydramine (DIP), fenpropidin (FEN), hydrochlorothiazide (HCT), lidocaine (LID), phenazone (PHE), sulpiride (SUL), tramadol (TRA), venlaflaxine (VEN). Other MPs with high ozone reactivity, for which no OTPs were detected, are: Benzophenone-3 (BZP), emtricitabine (EMT), metoprolol (MTO), mycophenolic acid (MYA), naproxen (NAP), ranitidine (RAN), resveratrol (RES).

(ii) Fast abatement of the MP with slow formation of the OTP

High abatement kinetics followed by a slow increase of the OTP is a typical indication for the formation of a secondary product, from an (un) detected primary product formed from the direct reaction with ozone. The secondary products still build up from the reaction of the (un) detected primary product with ozone and/or •OH, even though the target MP has been completely depleted.

A good example for this category is carbamazepine (CBZ, SI1) with its OTP BaQD (CBZ283). As discussed above, the fast oxidation of CBZ leads to the primary product BQM (CBZ251), which is then further oxidized to BQD (CBZ267) and finally to BaQD (CBZ283) (McDowell et al., 2005). The oxidation of BQD is a slow process, which leads to a continuous build-up of BaQD (CBZ283) until O3out. Further cases of this category are benzisothiazolone (BIT), sulfamethazine (SMZ) and sulfamethoxazole (SMX).

(iii) Intermediate abatement kinetics of the MP (non-detect or very low in the O_3 exposure range above 8×10^{-3} Ms and below 24×10^{-3} Ms) with a parallel OTP formation

Compounds with an intermediate ozone reactivity might react with ozone and •OH and the primary products can be formed from reactions with either ozone or •OH. Bezafibrate (BZF, SI1) is a representative compound with an intermediate ozone-reactivity ($k_{O3} = 590$ $M^{-1}s^{-1}$, at 20 °C (Huber et al., 2003)). If we assume the same activation energy as above (55 kJ/mol), a $k_{O3} = 188$ $M^{-1}s^{-1}$ at 6 °C can be calculated, leading to a predicted 80% abatement at an O_3 exposure of 8×10^{-3} Ms. This is close to the observed abatement of 82% at the same O_3 exposure. The main site of ozone attack is the alkoxybenzene moiety, which is controlling the ozone-reactivity. There are several products formed in parallel to its abatement during ozonation, which is an indication for their direct formation from the target MP possibly by •OH. MPs with similar reactivity patterns are caffeine (COF), methylprednisolone (MPN), propyzamide (PYZ), and sitagliptin (SIT).

(iv) Low abatement kinetics of the MP (still detectable at O_3 exposure of 24×10^{-3} Ms) with a parallel OTP formation.

Compounds with a low reactivity towards ozone, show low abatement kinetics during ozonation, which is mainly caused by the reaction with •OH. Atrazine (ATZ, SI1) is a classical case for this group of compounds with a $k_{O3} = 6$ $M^{-1}s^{-1}$ and $k_{OH} = 3 \times 10^9$ $M^{-1}s^{-1}$ at room

temperature (Acero et al., 2000). Under the experimental ozonation conditions in the pilot-plant, about 25% of its abatement is caused by a direct ozone reaction (calculated from overall ozone exposure until O3out), whereas 75% is due to reaction with •OH. Typical primary products were detected such as deisopropylatrazine (ATZ174) and deethylatrazine (ATZ188.0698) but also secondary products such as ATZ188.0334 and ATZ246. Several other compounds fall in this class, for which OTPs were detected: diuron (DIU), gabapentin (GAB), ibuprofen (IBU), lamotrigine (LAM), mecoprop (MEC), oxcarbazepine (OXC), prometon (PRM), sucralose (SUC), thiacloprid (THI), valsartan (VAL); or for which no OTPs were detected: 2,4-Dichlorophenoxyacetic acid (2,4-D), acesulfame (ACE), ketoprofen (KET).

3.1.4. Mechanisms of OTP formation

In the following sections the detected OTPs with their proposed structures and mechanisms of their formation will be discussed based on SI1 and SI2 for the different classes of MPs depending on their ozone-reactive functional groups and the compounds are ordered alphabetically for each functional group. The observed OTPs will be discussed based on mechanistic and kinetic understanding of ozone and •OH reactions mostly gained from controlled laboratory experiments in literature. Therewith, it is possible to test if the generally expected mechanisms occur within this empirical study under more realistic conditions at pilot scale.

In this section, the focus is on all 227 OTPs from 39 MPs, which are also summarized in SI1 and SI2, and all 51 parent compounds are discussed, even if no OTPs could be identified. The main components of these OTPs were detected in positive mode for 158 and in negative mode for 69 OTPs. The discussions include OTPs for which a formation mechanism can be proposed based on kinetic and mechanistic information. However, there are also numerous other OTPs for which the formation is unclear.

3.1.4.1. Tertiary amines. Cetirizine (CET, class i or ii): The abatement of CET as a function of the ozone exposure is very efficient (SI1 and SI2). At pH 7.8, CET reacts with an apparent second-order rate constant $k_{O3} = 2.4 \times 10^5\ M^{-1}s^{-1}$ with ozone at 20 °C (Borowska et al., 2016). The OTP CET217 has been detected in a previous mechanistic study from the direct ozone reaction with CET (Borowska et al., 2016). Even though it forms directly as a consequence of the abatement of CET, a further increase is observed even after CET is completely depleted. This points towards a formation of another primary product, e.g., the expected but non-detected *N*-oxide, which then further reacts to CET217. CET421, the second proposed product, is a *N*-oxide, which is expected from the direct ozone attack on the tertiary amine moiety (Borowska et al., 2016), but an additional oxygen is added. CET421 is formed rapidly but also shows a further formation after CET has been completely depleted. This points again towards a formation of a non-detected *N*-oxide followed by a secondary •OH attack on the rest of the molecule. In Borowska et al. (2016), the *N*-oxide was formed as major OTP in batch studies with •OH scavengers, but was also hardly found in ozonated wastewater, supporting the further transformation by •OH attack. From a kinetic point of view (intrinsic rate constants and number of carbons for •OH attack), a formation of a phenolic compound would be favorable, however, it would be abated very quickly to non-detect during the further ozonation. For example, phenol has an apparent $k_{O3} > 10^7\ M^{-1}s^{-1}$ at pH 8 and 20 °C (Hoigné and Bader 1983b). A reaction mechanism over a transient •OH-induced phenol formation from aromatic moieties, with a rapid further transformation by ozone, can be generally hypothesized for MPs or OTPs with low ozone reactivity. This will not be discussed in detail for each MP again. Therefore, in the case of CET421, a hydroxylation at the tertiary C-atom to a tertiary alcohol seems the most likely mechanism.

Citalopram (CIT, class i, Fig. 1): CIT is quickly abated during ozonation and CIT341 is the expected *N*-oxide, which is directly formed from CIT (SI1, SI2) (von Sonntag and von Gunten 2012). The secondary OTPs such as CIT245, CIT261, and CIT355 during ozonation of citalopram (CIT) are formed from CIT341, which is slowly oxidized by mostly •OH via various mechanisms, because no more ozone-reactive sites are present in CIT341. CIT261 and CIT355 are a result of an •OH attack to form a carbonyl group (-H2 + O) (von Sonntag and Schuchmann 1997) adjacent to the heterocyclic oxygen, CIT261 includes also a loss of the fluorobenzene ring. The next generation products (CIT277) includes a further *O*-addition to a hydroxylated species of CIT261, which is most likely again caused by •OH attack at the aliphatic side chains (von Sonntag and Schuchmann 1997), because a short-lived transient phenol moiety would escape detection.

Clarithromycin (CLA, class i): CLA is quickly abated with the formation of CLA764 (SI1, SI2), a *N*-oxide at the tertiary amine moiety, which has been previously reported ($k_{O3} = 4 \times 10^4\ M^{-1}s^{-1}$ at pH 7, 20 °C) (Lange et al., 2006; Merel et al., 2017). Once the *N*-oxide is formed,

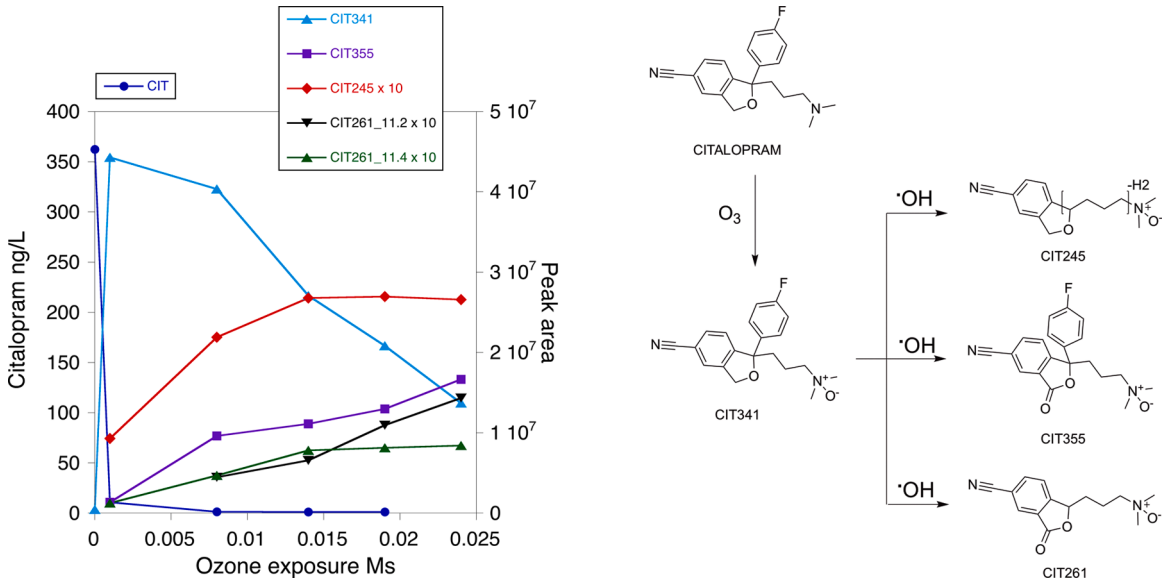

Fig. 1. Evolution of citalopram (class i) and OTPs during ozonation in the pilot plant (left) and the proposed reaction mechanisms for the formation of the OTPs (right). Some of the peak areas for the OTPs were multiplied by 10 for better comparison of the formation and abatement trends. The data points are mean values of three consecutive experiments. For further details see SI1 and SI2.

there are no more ozone-reactive moieties in this compound and CLA764 can only slowly be further abated by reactions with •OH. This leads to the formation of carbonyls from alcohols (CLA762) and hydroxylated species (CLA794) (von Sonntag and Schuchmann 1997). A second minor mechanism for tertiary amines involves an *N*-dealkylation (Zimmermann et al., 2012). The corresponding product is not observed, however a second generation acid (CLA606.3485, -H2 + O2) is formed by reactions with •OH (von Sonntag and Schuchmann 1997).

Diphenhydramine (DIP, class i): DIP is quickly abated with a formation of the *N*-oxide DIP272 by direct ozone reaction (SI1, SI2) (von Sonntag and von Gunten 2012). DIP210 is a secondary product, which is formed slowly most likely by •OH attack on the aromatic ring, which may lead to a loss of one of the benzene rings and formation of a carboxyl group via several reaction routes (Pan et al., 1993). The formation of DIP278 from the ozonation of DIP272 is characterized by a slow Criegee-type reaction on one of the aromatic rings ($k_{O3,benzene} = 2\ M^{-1}s^{-1}$ (Hoigné and Bader 1983a)), which might be enhanced by a transient phenol formation. The formation mechanism of DIP167 is unclear. It involves several reaction steps with •OH, finally leading to an intramolecular coupling. Coupling reactions of aromatic systems during ozonation have been observed before in low yields for phenol, mainly in experiments with relatively high parent compound concentrations (Mvula and von Sonntag 2003). This could be enhanced in the current study, because of the higher ozone stability of benzene and the proximity of the two benzene rings.

Fenpropidin (FEN, class i): Abatement of FEN leads to the primary *N*-oxide product (FEN290), which is formed quickly during ozonation (SI1, SI2) (von Sonntag and von Gunten 2012). Further OTPs from FEN290 are formed by an *O*-addition (FEN292, most likely alcohol formation at the aliphatic chain) and FEN320 with a mass difference of (-H2 + O2). The latter could be a result of a phenol formation with an ensuing further fast reaction to a benzoquinone by ozone (Ramseier and von Gunten 2009; Tentscher et al., 2018). Benzoquinones are less reactive with ozone ($k_{O3,benzoquinone} = 2.5 \times 10^3\ M^{-1}s^{-1}$ (Mvula and von Sonntag 2003)), which explains why this compound can still be detected during ozonation. Benzoquinones are toxicologically relevant OTPs, which need to be taken into consideration (Tentscher et al., 2018, Tentscher et al., 2021). A direct •OH attack on FEN leads to two carboxylated products (FEN288) and a benzoquinone (FEN304) (via a transient phenol), which undergoes further reaction to the *N*-oxide (FEN320).

Lidocaine (LID, class i, (Fig. 2): Also for this tertiary amine, the *N*-oxide (LID251) is the primary product (SI1, SI2) (von Sonntag and von Gunten 2012). The next generation OTP from the oxidation of LID251 by •OH is LID265, containing a carbonyl group (von Sonntag and Schuchmann 1997). Another product, LID221, is an imine *N*-oxide, formed via the *N*-desethyl-LID by ozone attack. LID221 is readily further degraded, which is expected for imine *N*-oxides ($k_{O3,N\text{-ethylethanimine oxide} \approx 1.9 \times 10^3\ M^{-1}s^{-1}$ at pH 7, room temperature) (Lim et al., 2019). The product of this reaction (LID207) is assumed to be the corresponding nitro compound (Lim et al., 2019), which has not been detected in this study. In contrast, the build-up and slow further reactions of LID249 (two products) show that the secondary amine is deactivated by a formation of amide-type compounds. They are formed by oxidation of one of the three carbon atoms adjacent to the N by •OH attack. Since there are two sites which lead to the same product and the third site is deactivated by an adjacent carbonyl group, it is proposed that the higher peak areas are related to LID249_13.4, whereas LID249_13.9 accounts for the other peak.

Sulpiride (SUL, class i): The N-oxide, SUL358 is directly formed by ozone attack (Merel et al., 2017), followed by the minor formation of SUL231 by cleavage of a side chain (SI1, SI2). Because of the low ozone reactivity of the amide nitrogen, the latter is probably formed by •OH attack. A C-N bond cleavage at the amide has also been observed for other MPs in this study (see below). For SUL359, the sulfonamide group in SUL358 is fully oxidized to a sulfonic acid, which is probably due to •OH attack (Lee et al., 2004).

Tramadol (TRA, class i): For TRA, again the *N*-oxide (TRA280) is the main OTP (Merel et al., 2017; Zimmermann et al., 2012) and the parent compound for further next generation OTPs, such as carbonyl compounds (TRA294_11.9/12.7) and alcohols (TRA296_10.7/11.8/12.1), which are formed by •OH attack on TRA280 (SI1, SI2). These products can further react by •OH attack to TRA310 and TRA328. Two further very minor TRA296_13.1/13.8 products are formed from an ozone attack on the anisole of TRA which has a $k_{O3} = 77\ M^{-1}s^{-1}$ at 22 °C (Zimmermann et al., 2012). TRA312 can either be formed from TRA280 by ozone attack on the anisole or from TRA296_13.1/13.8 by ozone attack on the tertiary amine moiety. The *N*-demethylated TRA has also been detected (TRA250), but it is expected to be formed only in minor quantities (Zimmermann et al., 2012). Further oxidation of TRA250 by •OH leads to several alcohols and carbonyl-type compounds (TRA264, TRA266). Some products have been formed from the •OH attack of TRA with an intact tertiary/secondary amine group. However, further reactions of these compounds with ozone are expected to lead to the corresponding *N*-oxides or nitro compounds (Lim et al., 2019; Zimmermann et al., 2012).

Venlafaxine (VEN, class i): VEN leads to a formation of the *N*-oxide by ozone attack (VEN294, (Lajeunesse et al., 2013; Lester et al., 2013;

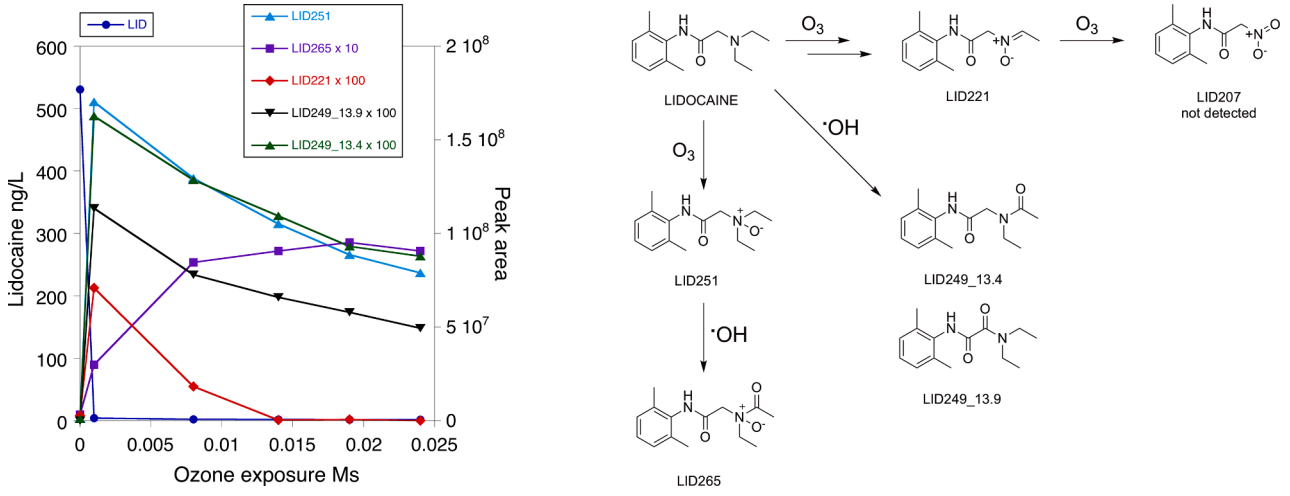

Fig. 2. Evolution of lidocaine (class i) and OTPs during ozonation in the pilot plant (left) and the proposed reaction mechanisms for the formation of the OTPs (right). Some of the peak areas of the OTPs were multiplied by 10 or 100 for better comparison of the formation and abatement trends. The data points are mean values of three consecutive experiments. For further details see SI1 and SI2.

Zucker et al., 2018)), which is followed by several OTPs formed by •OH attack, such as the alcohols VEN310 (three OTPs) and the carbonyls VEN308 (two OTPs) (SI1, SI2). VEN212 is a product formed by a loss of the cyclohexanol group induced by •OH attack. All these products still contain an anisole group, which reacts with ozone with k_{O3} = 290 $M^{-1}s^{-1}$ at 20 °C (Hoigné and Bader 1983a) and lead to their further abatement by direct ozone reaction to ring opening products (see TRA). If an activation energy of 55 kJ/mol is assumed (see Section 3.1.3), at 6 °C a $k_{O3,anisole}$ = 92 $M^{-1}s^{-1}$ can be calculated, which is very close to $k_{O3,VEN294}$ = 82 $M^{-1}s^{-1}$, which was calculated from the available abatement data. Since many of the OTPs have similar abatement patterns as VEN294, it can be concluded that their abatement kinetics is also controlled by an ozone attack on the anisole group. However, the expected ring opening products have not been detected, most likely because these more polar transformation products may not be retained on the SPE cartridge. An interesting side reaction is the formation of VEN292, an amide, which is recalcitrant at the nitrogen to further ozone attack. This compound reacts by •OH attack further to VEN308 (alcohol on hexyl ring) and by ozone at the anisole group to other products. Finally, also the *N*-demethylated form of VEN was detected (VEN264) and further oxidized to the amide (VEN278), which is then further abated by ozone attack on the anisole.

Overall, the observed ozonation mechanism of all discussed tertiary amines confirm that the following mechanism occur under the tested realistic set-up: The OTP formation of tertiary amines is initiated by the *N*-oxide formation, which was observed as main product for nearly all tertiary amines. The *N*-oxide formation is followed by further attack of ozone reactive moieties (e.g. anisole) by ozone. If we assume second-order rate constants of k_{O3} = 100 $M^{-1}s^{-1}$ and k_{OH} = 5 × 10^9 $M^{-1}s^{-1}$ for the second reactive site (e.g., anisole) and a $R_{ct} = 10^{-8}$, the fraction of the ozone reaction is 67%. Therefore, both ozone- and •OH-induced higher generation products are possible. If no further ozone-reactive sites are present, the reactions proceed by •OH attack. Generally, a preferential site of •OH attack are aromatic moieties. However, due to the fast ozone reactions of the formed phenolic moieties, they escape detection. Nevertheless, some potential ring opening products were detected, which could be the result of ozone attack on the transient phenols and support the occurrence of this reaction. If no aromatic sites are present in the MPs or OTPs, •OH attack occurs at aliphatic carbons leading mostly to alcohols and carbonyls, which are often detected as secondary products.

3.1.4.2. Secondary amines. Atenolol (ATE, class i): Several products are formed directly from ATE by ozone attack at the secondary amine (k_{O3} = 10^4 $M^{-1}s^{-1}$ at pH 7.8, 20 °C) and the anisole moieties (k_{O3} = 110 $M^{-1}s^{-1}$ at pH 7.8, 20 °C) (Benner et al., 2008) (SI1, SI2). The first detected product ATE299 is a result of an ozone attack on the anisole moiety with the ensuing formation of the muconaldehyde-type compound (Criegee-type reaction), even though the formation of an imine oxide from an ozone attack on the secondary amine would be kinetically favorable. This non-detected product is an intermediate to the nitro compound ATE255, which is the expected end product from the reaction with ozone (k_{O3} = 1.9 × 10^3 $M^{-1}s^{-1}$ at pH 7.0, 20 °C) (Lim et al., 2019; Shi and McCurry 2020). For a detailed discussion of the kinetics, see Section 3.1.3.

Flecainide (FLE, class i, Fig. 3): FLE should react at the dialkoxybenzene ring with a k_{O3} = 1.3 × 10^5 $M^{-1}s^{-1}$ for dimethoxybenzene (SI1, SI2) (Munoz and von Sonntag 2000). However, the trifluoromethyl groups may reduce the reactivity of the aromatic ring. Nevertheless, the observed abatement kinetics of FLE with an estimated $k_{O3} \approx 700$ $M^{-1}s^{-1}$ points toward this site, because it is significantly more reactive than the piperidine-*N* of FLE with a $k_{O3} \approx 70$ $M^{-1}s^{-1}$ at pH 7.8, 20 °C (Tekle-Röttering et al., 2016a). Nevertheless, no products were identified from the reaction of ozone at the aromatic ring, because they probably escape detection by the applied analytical procedure. FLE429, which is most likely an imine *N*-oxide from an ozone attack on the secondary amine, has been postulated as an intermediate for the oxidation of secondary amines to nitro compounds (Lim et al., 2019). The further reaction of FLE429 proceeds with an estimated (from pilot plant data) $k_{O3} \approx 300$ $M^{-1}s^{-1}$, which is about a factor of two lower than

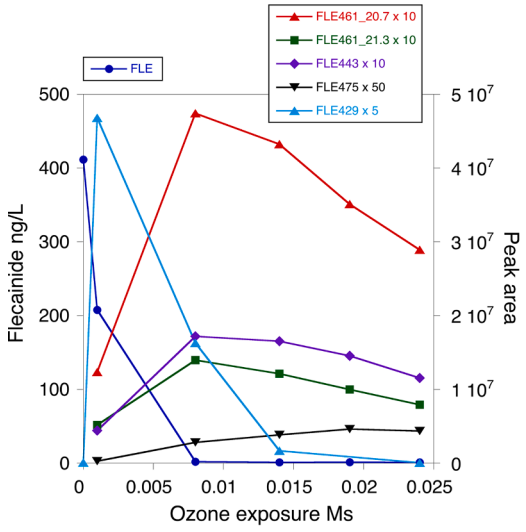

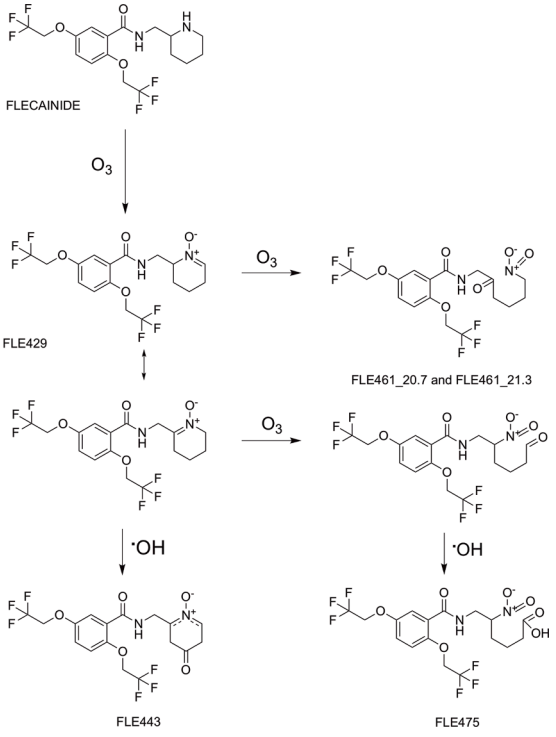

Fig. 3. Evolution of flecainide (class i) and OTPs during ozonation in the pilot plant (left) and the proposed reaction mechanisms for the formation of the OTPs (right). Some of the peak areas of the OTPs were multiplied by 5, 10 or 50 for better comparison of the formation and abatement trends. The data points are mean values of three consecutive experiments. For further details see SI1 and SI2.

for the analogous imine *N*-oxide of aliphatic amines (k_{O3} = 608 $M^{-1}s^{-1}$ for *N*-ethylethanimine oxide calculated at 6 °C (Lim et al., 2019)). However, such differences between an aliphatic and a cyclic imine *N*-oxide seem possible. The ensuing products are two nitro compounds with a ring opening on both sides of the imine oxide group and a carbonyl group (FLE461). The next generation product (FLE475) is formed by an •OH attack on the carbonyl carbon to form an acid. The formation of FLE443 occurs by •OH attack on the piperidine moiety of FLE429 with the formation of a carbonyl moiety.

Metoprolol (MTO, class i): MTO has a very similar abatement profile as ATE, which is expected from similar reactivities with ozone (Benner et al., 2008). However, in this case no OTPs were observed (SI1, SI2).

Overall, secondary amines react to the expected formation of the *N*-nitro compounds via the intermediate imine oxide, which is not always detected. If additional ozone-reactive sites are present (e.g. activated aromatic moieties), some of the ensuing products have also been detected. In absence of such moieties or if they are already oxidized, further reactions with •OH lead to alcohol- and carbonyl-type compounds.

3.1.4.3. Primary amines. Gabapentin (GAB, class iv): For gabapentin (GAB, k_{O3} = 15 $M^{-1}s^{-1}$, pH 7, (Bourgin et al., 2017)) only one OTP was observed, which is formed directly from •OH attack on the cyclohexyl moiety with the ensuing formation of a carbonyl group (GAB186) (SI1, SI2). The expected nitro compound from the attack of ozone at the primary amine was not observed.

Sitagliptin (SIT, class iii): Sitagliptin with a $k_{O3} = 1.8 \times 10^3$ $M^{-1}s^{-1}$ at pH 8, 20 °C (Hermes et al., 2020) is abated somewhat more efficiently than other class (iii) compounds like BZF and MPN (see below), with direct and continuous formation of several products, from which SIT436 is highlighted, because it is the expected formation of a nitro-compound from the primary amine group (SI1, SI2) (Lim et al., 2019; Shi and McCurry 2020). Another OTP (SIT422) results from an •OH attack on the three methyl groups of the aliphatic heterocycle to form carbonyl (amide)-type compounds (Hermes et al., 2020). The exact location of the carbonyl group is unknown. Several other primary and secondary products have been observed and also partially described in literature, however, the mechanisms of their formation are currently unclear.

Overall, the compound basis for the assessment of primary amines was quite small. Nevertheless, the expected formation of a nitro compound could be verified in the case of SIT.

3.1.4.4. Olefins. Carbamazepine (CBZ, class i): The kinetics of the reactions of CBZ have been discussed in Section 3.1.3. There are several previous product studies on the transformation of CBZ during ozonation (Azaïs et al., 2017; Hübner et al., 2014; Kråkström et al., 2020; McDowell et al., 2005). The primary and fast ozone attack occurs at the olefin moiety and leads to a ring opening with a secondary ring formation (CBZ251), followed by further oxidations to CBZ267 and CBZ283 (SI1, SI2). Further products (CBZ163, CBZ179) formed from an •OH attack were detected here and in another study (Azaïs et al., 2017). We suggest that the previously proposed structure CBZ179 is incorrect, because a phenolic compound has been proposed with an expected fast ozone reaction, which would make its detection unlikely. Therefore, we suggest a hydroxylamide-type structure for CBZ179. The evidence of our MS^2 spectrum is not specific enough and fits to both structures. From the build-up pattern, CBZ163 and CBZ179 seem to be formed from CBZ251 by ozone/•OH attack on the pyrimidine ring and a cleavage of the C-N bond of the amide-type moiety. Furthermore, CBZ136 and CBZ207, previously detected OTPs, are formed (Azaïs et al., 2017), however, no detailed mechanism is available. In a recent study, an even broader range of OTPs was proposed (Kråkström et al., 2020).

Caffeine (COF, class iii): The intermediate reactivity of COF with ozone (k_{O3} = 650 $M^{-1}s^{-1}$ at pH 8.1, 20 °C (Broséus et al., 2009)) warrants a direct ozone reaction. COF has been classified as an olefin, present in the imidazole-type group, which reacts with ozone at the C-C double bond to ring opening products (Tekle-Röttering et al., 2020). However, the observed OTP (COF225) does not result from this reaction but an addition of two oxygen atoms (SI1, SI2). This OTP has been reported previously under alkaline conditions in absence of a scavenger for •OH, hence, it is probably formed by •OH attack (Rosal et al., 2009).

Methylprednisolone (MPN, class iii): The second-order rate constant for the reaction of MPN with O_3 is unknown, however, it is structurally similar to progesterone, which contains also an olefin with an α-carbonyl group (k_{O3} = 480 $M^{-1}s^{-1}$, 18 °C (Barron et al., 2006)). MPN reacts via a Criegee-type mechanism with ozone to form a product with two aldehyde moieties. This product has not been detected, however, two further oxidation products were observed (SI1, SI2): MPN393, which has, besides the additional aldehyde moieties, a cleaved methanol group and an added hydroxyl group at one of the aliphatic carbon sites, and MPN437, for which the primary product has been oxidized at the aldehyde to form a carboxylic acid by reactions with •OH.

Phenazone (PHE, class i): PHE165 is formed directly from the parent compound by the fast reaction of ozone with phenazone ($k_{O3} = 5 \times 10^4$ $M^{-1}s^{-1}$ for aminophenazone (Zhang et al., 2015)) (SI1, SI2). Compared to pyrazole (k_{O3} = 56 $M^{-1}s^{-1}$ (Tekle-Röttering et al., 2020)), the reactivity of PHE is much enhanced, due to conjugation with the aromatic ring. The product formation (PHE165) occurs by an initial Criegee-type reaction with an ensuing cleavage of the N-C(=O) bond by hydrolysis. This hydrolyses might also occur during storage of the samples. PHE179 is formed by •OH attack on the methyl group of N-CH_3.

Propyzamide (PYZ class iii): PYZ has an ethinyl group as the main ozone-reactive site with k_{O3} = 160 $M^{-1}s^{-1}$ at 10 °C based on 1-ethinyl-1-cyclochexanol (Huber et al., 2004). Two main OTPs from the ozone-attack on the ethinyl group are directly formed from PYZ (PYZ301, PYZ320) (SI1, SI2). PYZ320 may also be further transformed to PYZ301. PYZ274 is formed by decarboxylation of PYZ301.

Overall, it could be confirmed that the main site of primary attack of olefins and ethinyl groups are the C-C double or triple bonds, respectively, with the formation of the corresponding carbonyl and acid groups. In the special case of CBZ, a secondary ring formation has been observed.

3.1.4.5. Aromatic compounds. 2,4-Dichlorophenoxyacetic acid (2,4-D, class iv): 2,4-D does not have any ozone reactive sites and will be abated by •OH. No OTPs were detected from this compound (SI1, SI2). This is probably again due to the formation of phenolic compounds by •OH attack, which are then rapidly abated by ozone to muconic-type compounds, which escape detection.

Bezafibrate (BZF, class iii, Fig. 4): BZF240 is the product of two Criegee-type attacks on the alkoxy aromatic moiety (Sui et al., 2017) (SI1, SI2). Thereafter, several products are formed from an •OH attack, initially BZF254 (acid from aldehyde) followed by the BZF212 (by decarboxylation), BZF226 (acid from aldehyde) and finally BZF196 (Dantas et al., 2007). BZF254 can also be formed via formation of a phenol by an initial •OH attack, followed by a Criegee-type ring cleavage of the activated aromatic system. The pathway to BZF256 is currently unclear, but is most likely a combination of ozone and •OH reactions. BZF156, which has been previously reported (Sui et al., 2017), is again a result of an •OH-induced cleavage of the C-N bond of the amide group, which has been observed for several other compounds in this study. BZF376 formation is a consequence of a direct •OH attack on BZF (Rivas et al., 2019). This OTP cannot unambiguously be assigned to a structure, but an addition of an OH-group on one of the aliphatic carbons is assumed.

Benzophenone-3 (BZP, class i): Due to the phenolic moiety its abatement by ozone is very fast (see cetirizine) (SI1). This is a confirmation that even if phenolic compounds were formed, their lifetime would be too short to be detected. Furthermore, since there were no OTPs detected for this compound, this is another indication that such OTPs

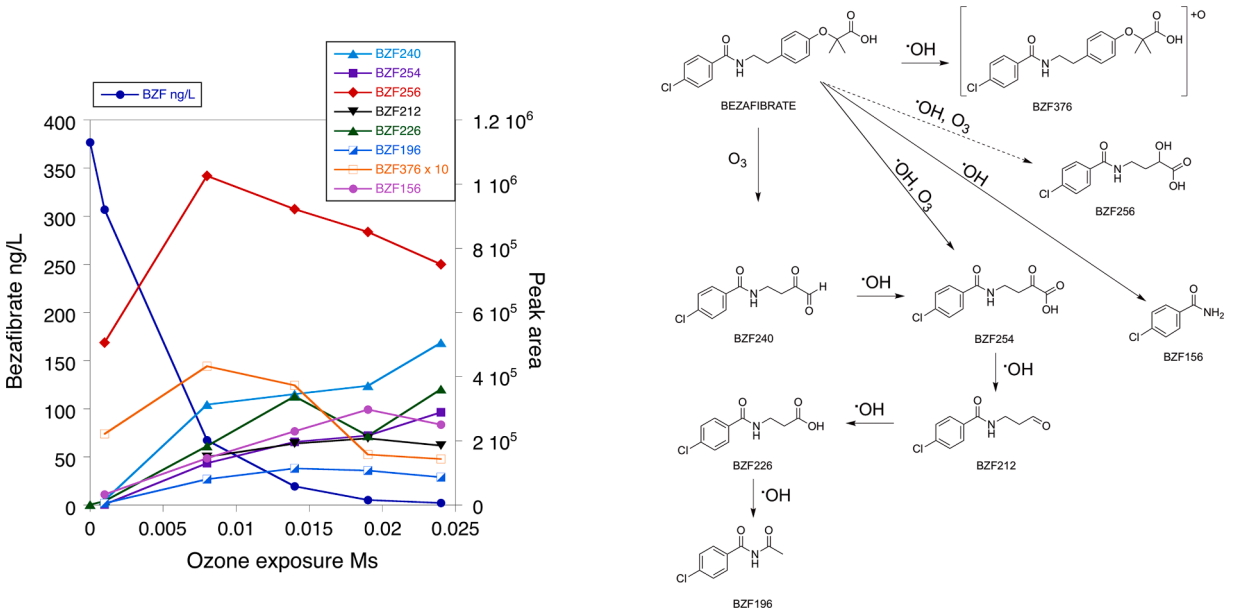

Fig. 4. Evolution of bezafibrate (class iii) and OTPs during ozonation in the pilot plant (left) and the proposed reaction mechanisms for the formation of the OTPs (right). The peak area of BZF376 was multiplied by 10 for better comparison of the formation and abatement trends. The data points are mean values of three consecutive experiments. For further details see SI1 and SI2.

(most likely ring-opening products from phenol oxidation) escape our analytical procedure.

Benzotriazole (BZT): BZT could not be quantified and no OTPs were detected for this compound.

Diclofenac (DIC, class i): DIC reacts with a $k_{O3} = 6.8 \times 10^5 - 1 \times 10^6$ $M^{-1}s^{-1}$ with ozone at room temperature (Huber et al., 2003; Sein et al., 2008). Based on its formation profile, DIC282 is the primary OTP with a loss of CH_2 relative to DIC (SI1, SI2). An ozone attack on the DIC-nitrogen has been proposed previously (Sein et al., 2008). However, it is unclear how this may lead to a loss of CH_2. Furthermore, based on high second-order rate constants for the reaction of hydroxylamines with ozone (Lim et al., 2019), it should be detected in only very low concentrations. Based on its formation trend, DIC259 is a secondary OTP formed by two Criegee-type reactions with a loss of four carbon atoms. This product is then further transformed by another Criegee-type reaction and a decarboxylation to DIC189, which was detected previously (Coelho et al., 2009).

Hydrochlorothiazide (HCT, class i): HCT is a special sulfonamide, which reacts fast with ozone to chlorothiazide (HCT295) by electron transfer (SI1, SI2) ($k_{O3} \approx 3 \times 10^5$ $M^{-1}s^{-1}$ at pH 8 (Borowska et al., 2016)). This can be slowly oxidized to the secondary OTP HCT311 and finally to HCT313 and HCT341 in very low yields (Borowska et al., 2016).

Mecoprop (MEC, class iii-iv): The kinetics of MEC abatement is between group (iii) and (iv) with a $k_{O3} \approx 100$ $M^{-1}s^{-1}$ (Beltran et al., 1994). Only one OTP (MEC227) was observed, which is formed by •OH attack at the toluene methyl group (SI1, SI2). Other expected products from an •OH attack on the aromatic ring with the ensuing phenol formation will escape detection (see cetirizine).

Naproxen (NAP, class i): The alkoxynaphtalene group reacts quickly with ozone, with $k_{O3} \approx 10^5$ $M^{-1}s^{-1}$ (Benner et al., 2008). No products were found, similar to some of the other fast-reacting aromatic compounds.

Sulfamethoxazole (SMX, class ii): Only secondary products were detected for SMX (SI1, SI2). SMX282, the nitro-SMX, has also been detected in previous studies (Abellan et al., 2008; Gao et al., 2014; Willach et al., 2017) and is expected to be formed via the corresponding hydroxylamine (Lim et al., 2019; Willach et al., 2017). This OTP has a much lower expected ozone-reactivity ($k_{O3,nitrobenzene} = 0.09$ $M^{-1}s^{-1}$ (Hoigné and Bader 1983a)). Therefore, no further ozone reaction products from the nitrobenzene moiety were detected. SMX200, a subsequent product from the oxidation of SMX282, is also formed from SMZ (see below). It results from a cleavage of the N-C bond of the sulfonamide group, similar to several other observations of N-C bond cleaved of amides. SMX225 has been reported as a potential OTP for the electrochemical transformation of SMX (Martín de Vidales et al. 2012). Therefore, this is most likely an OTP that is formed by •OH attack on SMX282.

Sulfamethazine (SMZ, class ii): Based on the formation profiles of the OTPs, only secondary and later generation OTPs are detected for SMZ (SI1, SI2). For SMZ, the same secondary product (SMZ200) is formed as for SMX (see above) via oxidation of the aniline to a nitrobenzene and a slow cleavage of the sulfonamide N-C bond. It is unclear why the nitro-SMZ was not detected in analogy to the nitro-SMX (SMX282). SMZ144 is the result of a N-S bond cleavage and an ozone- or an •OH-attack with ring opening of the pyrimidine (Tekle-Röttering et al., 2016b). This is expected to be a very slow process due to a low ozone- and •OH-reactivity of the pyrimidine moiety ($k_{O3} < 0.5$ $M^{-1}s^{-1}$, $k_{OH} = 1.6 \times 10^8$ $M^{-1}s^{-1}$) (Buxton et al., 1988; Tekle-Röttering et al., 2016b).

Trimethoprim (TRI, class i): TRI contains two reactive sites and at pH 7.8, the heterocyclic ring is the main moiety of ozone attack ($k_{O3} = 4.3 \times 10^5$ $M^{-1}s^{-1}$ (Dodd et al., 2006)). Nevertheless, also the trimethoxybenzene moiety reacts quickly with ozone ($k_{O3} \approx 8 \times 10^4$ $M^{-1}s^{-1}$ (Dodd et al., 2006)). Based on the loss of C5H6, the detected OTP (TRI225) is likely a result of ozone-attacks on the trimethoxybenzene moiety and the other products escape detection (SI1, SI2).

Overall, (activated) aromatic compounds react quickly with ozone and it seems difficult to detect the ensuing OTPs. When OTPs were identified, often a ring opening is observed and it can be assumed that such products become too polar and escape the enrichment procedure. For aniline-type compounds, OTPs with nitro groups have been detected. Electron transfer is another option of reactions of aromatic compounds with ozone. The only example with direct evidence for this reaction path is hydrochlorothiazide. Furthermore, aromatic compounds reacting with •OH are expected to yield phenolic compounds, which react too quickly with ozone to be detected under the given experimental conditions. Also, the expected ring opening products from the ensuing ozone reactions were rarely detected in this study.

3.1.4.6. Sulfur-containing compounds. Benzisothiazolone (BIT, class ii): There is no second-order rate constant available for the BIT-ozone reaction, however, reduced sulfur species typically react readily with ozone to the corresponding sulfoxide (von Sonntag and von Gunten 2012), which can explain the fast abatement of this target compound during ozonation in the pilot plant (SI1, SI2). The further reaction of the sulfoxide by ozone to a sulfone-type compound is much slower ($k_{O3} = 8$ $M^{-1}s^{-1}$ for DMSO (von Sonntag and von Gunten 2012)), which would lead to the continuous increase of the corresponding product. For BIT, the formation of sulfoxide was not observed, but the formation of the sulfone-type product (BIT181), which has also been detected previously (Li et al., 2016). However, a significantly higher $k_{O3} \geq 250$ $M^{-1}s^{-1}$ for the reaction of the sulfoxide with ozone would be necessary to explain the relative fast increase of BIT181. Compared to DMSO, a higher second-order rate constant for the reaction of BIT-sulfoxide can be expected due to the conjugation with the aromatic ring, however, its magnitude is unknown. BIT215 (Cl-adduct of BIT179 with a mass difference of -H2 - O2), the second detected OTP, is proposed to result from an $^{\bullet}$OH attack on the aromatic ring to form a phenol with an ensuing reaction with ozone to the benzoquinone (Ramseier and von Gunten 2009; Tentscher et al., 2018).

Emtricitabine (EMT, class i): EMT is abated very quickly during ozonation due to an ozone attack at the thioether group (SI2) ($k_{O3,\ methionine} = 4 \times 10^6$ $M^{-1}s^{-1}$ (Pryor et al., 1984)). No OTPs were detected in this case, however, the formation of a sulfoxide can be expected as a primary product (Dodd et al., 2010).

Overall, with only two examples in this group, it is difficult to draw general conclusions. Nevertheless, due to the high reactivity of thioether groups the formation of sulfoxide- and sulfone-type OTPs can be expected.

3.1.4.7. Compounds with several ozone-reactive moieties. Clindamycin (CLI, 3°amine and thioether, class i): The primary OTP is CLI457, which contains a *N*-oxide and a sulfoxide, resulting from the parallel ozone reactions at the 3° amine and the thioether (SI1, SI2). The reactivity of CLI is expected to be very similar to lincomycin with $k_{appO3,N} = 1.58 \times 10^6$ $M^{-1}s^{-1}$ and $k_{appO3,S} = 3.26 \times 10^5$ $M^{-1}s^{-1}$ at pH 8, room temperature (Qiang et al., 2004). Since both k_{O3} are very high under the experimental conditions at the pilot plant, the OTPs with ozone attack at only one site escape detection. CLI457 reacts slowly by $^{\bullet}$OH attack to several carbonyl compounds (CLI427, CLI471). Further products (e.g., *N*-demethylated CLI, with a loss of sulfur (CLI381)), were also detected, however, no mechanistic interpretation of these findings is currently available. Further OTPs from CLI381 are formed by $^{\bullet}$OH attack to a carbonyl (CLI395) and an alcohol (CLI397). CLI187 are two products formed from a C-N bond cleavage of the amide group followed by a formation of two alcohols on the cyclic structure. These reactions are induced by $^{\bullet}$OH attacks.

Cephalexin (CPX, olefin, thioether and 1° amine, class ii): Under the experimental conditions in this study, CPX reacts quickly with ozone ($k_{O3} = 9.1 \times 10^4$ $M^{-1}s^{-1}$ at pH 7.7 at room temperature (Dodd et al., 2006)) (SI1, SI2). In an ozonation study, the main identified products were sulfoxide and carbonyl compounds resulting from the ozone-attack on the thioether and the olefin (Dodd et al., 2010). The attack at the 1° amine moiety is quite a bit slower (Lim et al., 2019). The detected OTP in this study (CPX165) is not a primary product (increase after full depletion of the target compound), but the result of other OTPs (nitroso moiety resulting from an ozone attack on the primary amine (Lim et al., 2019)). CPX165 also is a result from a cleavage of the C-N bond at the amide group, likely induced by $^{\bullet}$OH attack, as described previously.

Mycophenolic acid (MYA, olefin and activated aromatic moiety, class i): MYA is expected to have a very high reactivity with ozone, with a primary attack at the phenol moiety and a secondary attack at the olefin. Since both reactions are fast, an OTP with products on both sites is expected, similar to CLI. The OTP is expected to be very polar and might escape the enrichment procedure. Therefore, no OTP was detected for MYA (SI2).

Oseltamivir (OSE, olefin and 1°amine, class i): In analogy to the reaction of oseltamivir acid with ozone, it is expected that the olefin is the main moiety of attack ($k_{O3} = 1.7 \times 10^5$ $M^{-1}s^{-1}$ at pH 7–8 at room temperature (Mestankova et al., 2012)). The two OTPs OSE303 are a result of this reaction, but with an additional loss of C_2H_2 and addition of O (SI1, SI2). The formation of a second 1° amine is proposed by an $^{\bullet}$OH-induced bond cleavage of the acetyl group. One of the OSE303 products could be a result of a secondary ring formation, the other with the two free amine groups. Both OSE303 are abated similarly, probably due to an ozone attack on the primary amine moiety, possible leading to a nitro compound (OSE343). OSE359 is an OTP with a bond cleavage of the olefin and an oxidation of the primary amine to the corresponding nitroso compound (Lim et al., 2019).

Propranolol (PRO, 2°amine and activated aromatic moiety, class i): The ozone reactivity of PRO at pH 7.8 is governed by the attack on the alkoxynaphtalene moiety ($k_{O3} \approx 10^5$ $M^{-1}s^{-1}$ at pH 7.8 (Benner et al., 2008)), leading to a Criegee-type ring opening product. This product escapes the analysis because the reaction of the secondary amine with ozone to PRO308 is still sufficiently fast ($k_{O3} \approx 1.7 \times 10^4$ $M^{-1}s^{-1}$ (Benner et al., 2008)) (SI1, SI2). PRO308 has been reported previously to be an OTP of PRO (Benner and Ternes 2009). Since it is a hydroxyl amine, it is expected to be quickly further oxidized to the ensuing nitro compound, which was not detected in this study.

Ranitidine (RAN, 3°amine, thioether and furan moiety, class i): The abatement of RAN is very fast and likely, products are formed with multiple ozone attacks at various sites. None of them were detected in this study (SI2).

Resveratrol (RES, resorcinol, phenol and olefin, class i): RES is expected to react with ozone at multiple sites and likely small molecular weight OTPs will be formed, which may escape enrichment and/or detection (SI2).

Overall, for compounds with several reactive sites, often the time resolution in the pilot ozonation experiments is not sufficient to find OTPs from the reaction at only one site. Some OTPs from multiple ozone attacks are detected, others may escape detection since they are small and polar.

3.1.4.8. Compounds with low ozone reactivity. Acesulfame (ACE, olefin, class iv): ACE contains a deactivated olefin group ($k_{O3} = 88$ $M^{-1}s^{-1}$, 20 °C (Kaiser et al., 2013)), which is the ozone-reactive site of this compound. The Criegee-type ring opening product has been proposed previously with an ensuing hydrolysis to smaller detected compounds (Scheurer et al., 2012). However, detection of these low molecular weight compounds is unlikely with the applied analytical procedure in the current study, and therefore, no OTPs were detected (SI2).

Atrazine (ATZ, class iv): The kinetic features of ATZ are discussed in Section 3.1.3 and are controlled by mostly $^{\bullet}$OH reactions. Typical previously reported products were detected such as deisopropylatrazine (ATZ174), deethylatrazine (ATZ188_17.1), 4-acetamido-2-chloro-6-isopropylaminos-triazine (CDIT, ATZ230), 4-acetamido-2-chloro-6-ethylaminos-triazine (CDET, ATZ216) and 4-acetamido-6-amino-2-chloro-s-triazine (CDAT, ATZ188_12.0) (SI1, SI2) (Acero et al., 2000; Barletta et al., 2003; Beltrán et al., 1998). The imine-type compounds, which are formed in high yields from both ozone and $^{\bullet}$OH reactions, were not identified, because they hydrolyse with half-life times in the order of 4 h at pH 8 and result in the formation of many of the detected OTPs (Acero et al., 2000). Another secondary product (ATZ212) has been detected and is formed by an OH substitution of the Cl on the triazine ring. Even though this product has not been reported during ozonation, an $^{\bullet}$OH attack has been demonstrated previously on the triazine ring, which may eventually lead to the formation to a hydroxylated OTP (Tauber and von Sonntag 2000).

Diuron (DIU, class iv): DIU reacts with a $k_{O3} = 16.5$ $M^{-1}s^{-1}$ with

ozone and lies between class (iii) and class (iv) (Benitez et al., 2007). Its primary OTP DIU216 is the dealkylated secondary amide, which is formed by •OH attack (Solís et al., 2016) and is another example of a cleavage of a C-N bond of an amide group (SI1, SI2). Substitution of Cl by OH through •OH attack has been reported before during ozonation, with the formation of DIU215 (Feng et al., 2008; Solís et al., 2016). However, the corresponding phenol-type compound should be abated more readily than observed in the pilot-plant ozonation as demonstrated by the tested phenolic target compounds, e.g. benzophenone-3 (Hoigné and Bader 1983b). It is unclear why this does not happen. DIU199 is a secondary product most likely formed from DIU216. Another product with unknown structure (DIU201) has also been formed.

Ibuprofen (IBU, class iv): Ibuprofen (IBU) has a similar ozone-reactivity as ATZ (k_{O3} = 9.6 $M^{-1}s^{-1}$ (Huber et al., 2003)) and two direct products have been detected (IBU221, IBU240) (SI1, SI2). They are most likely both results of •OH-attacks.

Ketoprofen (KET, class iv): Ketoprofen, which has two non-activated benzene rings, is expected to have a low ozone-reactivity. Therefore, it will mostly be abated by •OH, which possibly leads to a transient formation of phenolic compounds, which then are abated very quickly by direct ozone reactions to products escaping detection (SI2).

Lamotrigine (LAM, class iv): The abatement of lamotrigine (LAM, k_{O3} ≈ 4 $M^{-1}s^{-1}$ (Keen et al., 2014)) is very similar to ATZ, which means that •OH play an important role in OTP formation. The two OTPs LAM254 and LAM259 were previously described during ozonation of LAM (SI1, SI2) (Bollmann et al., 2016; Keen et al., 2014). Even though an OH addition on the aromatic ring has been described before (Keen et al., 2014), the formation of a phenolic compound (LAM272) is very unlikely and it should not be detectable (see cetirizine) (Hoigné and Bader 1983b). Therefore, an alternative for LAM272 is the formation of an *N*-oxide, which should be much more recalcitrant towards further oxidation (Bollmann et al., 2016), which is demonstrated by a steady increase of this OTP.

Metformin (MET, class iv): MET could not be quantified in this study and no OTPs were detected.

Oxcarbazepine (OXC, class iv): Even though there is no k_{O3} available for this compound, it is expected to react slowly with ozone. OXC238 is the only OTP detected and it is hypothesized that a loss of the amide group and a formation of a carbonyl-type compound occurs by •OH-attack (SI1, SI2). OXC238 is an aniline-type compound which reacts quickly with ozone, which is reflected in the fast abatement of this OTP.

Prometon (PRM, class iv): PRM, which has a triazine structure, leads to analogues OTPs as ATZ, which are mostly formed by •OH attack, such as deisopropyl-PRM (PRM184) and PRM240, with a carbonyl group at the methyl-C (SI1, SI2). Further, •OH oxidation of the latter leads to carboxylic acid PRM256. PRM142, the OTP without the isopropyl groups, is also detected and is slowly formed from PRM184. Several other products are formed from •OH reactions.

Sucralose (SUC, class iv): SUC has a very low reactivity with ozone (k_{O3} < 0.1 $M^{-1}s^{-1}$ (Bourgin et al., 2017)) and reacts mostly with •OH, even though the corresponding k_{OH} = 1.56 × 10^9 $M^{-1}s^{-1}$ is quite low as well (Keen and Linden 2013). During the UV/H_2O_2 process, several products with substitution of Cl by OH have been identified (Keen and Linden 2013), however, the structure of SUC376 is currently unclear (SI1, SI2). The formation of an olefin-type OTP was previously proposed (Gulde et al., 2021, Keen and Linden 2013), however, the steady formation of SUC376 during ozonation contradicts this assumption. An olefin would escape detection, because its abatement is faster than its formation.

Thiacloprid (THI, class iv, Fig. 5): The primary product is THI283, with the thioether oxidized to a sulfone group (SI1, SI2). Since the reaction kinetics are relatively low, it is expected that this occurs via •OH attack. It seems that the thioether group is deactivated in this compound. Based on the patterns of the other OTPs, it can be assumed that they are secondary products from THI283. One case in point is the loss of SO2 from THI283 to THI251. Further reactions with a loss of CH2S or C2H2S lead to the products THI237 or THI211, respectively. The corresponding hypothesized structures are provided in Fig. 5. For THI211, two products with different retention times were detected, only one of them is proposed in the mechanism in Fig. 5.

Valsartan (VAL, class iv): Sartan-type compounds are known to be quite stable during ozonation (Bourgin et al., 2018). Based on the low measured reactivity of irbesartan, a structurally similar compound (k_{O3} = 23 $M^{-1}s^{-1}$ (Bourgin et al., 2018)), and a simulated k_{O3} ≈ 34 $M^{-1}s^{-1}$ for VAL (Lee et al., 2014), it is abated similarly to IBU and it can be assumed that VAL reacts mostly with •OH. An interesting case is VAL280, which degrades quickly after its formation (SI1, SI2). This is an indication that VAL280 has a higher ozone reactivity than the parent compound (k_{O3} ≈ 200 $M^{-1}s^{-1}$, calculated based on the abatement of VAL280). This could be due to the formation of a secondary amine (k_{O3} ≈ 800 $M^{-1}s^{-1}$ at pH 7.8 and 20 °C (Lim et al., 2019)) for which a lower k_{O3} in the order of the calculated value at 6 °C can be assumed.

Overall, the product formation of MPs with low ozone-reactivity is governed by •OH reactions, which may lead to a much broader product

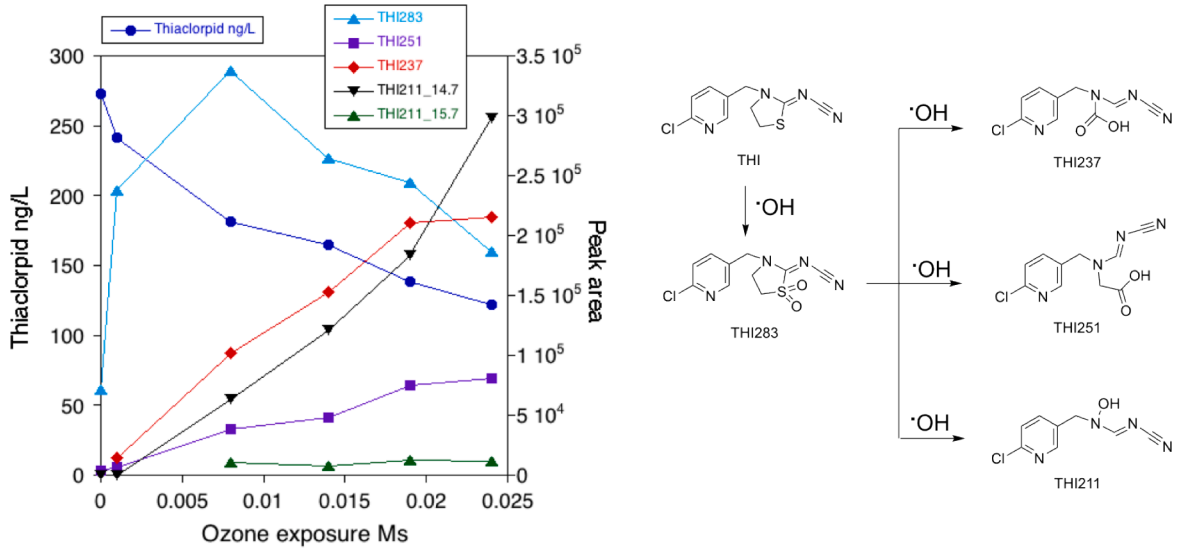

Fig. 5. Evolution of thiacloprid (class iv) and OTPs during ozonation in the pilot plant (left) and the proposed reaction mechanisms for the formation of the OTPs (right). The data points are mean values of three consecutive experiments. For further details see SI1 and SI2.

distribution. For non-activated aromatic compounds, phenolic moieties may be formed, which are extremely short-lived. In one case the formation of an aniline-type compound was observed, which is then also quickly abated by direct reaction with ozone.

3.1.5. Bromate formation

Bromate increased linearly as a function of the contact in the ozonation reactor. Since the bromide level was low (12–15 μg/L), the maximum bromate concentration at O3out was only about 2 μg/L (Fig. S7, SI3), which is well below the drinking water standard of 10 μg/L (WHO 2017). The bromate level increased in the sand filter, because there was still a significant ozone residual concentration at O3out (Fig. S3, SI3). Ozone was completely depleted in the first 10 cm of the sand filter (Fig. S3, SI3) and bromate still increased in this part of the filter to approximately 3.5 μg/L. As expected, bromate was not degraded in the sand filter, because it is only biodegradable under denitrifying conditions, which are not common after ozonation with a high residual oxygen concentration (Hijnen et al., 1995).

3.2. Pilot-scale sand filter

3.2.1. General considerations

A post-treatment with a biologically active sand filter was tested to elucidate the abatement of OTPs relative to their parent compounds. Such a treatment often follows ozonation to improve the biostability of the water by degradation of bioavailable bulk organic matter produced in ozonation and it is often assumed that OTPs are also well abated during this treatment step.

To test the biological activity of the sand filter, four test compounds with known biodegradability were dosed to the filter inlet and their abatement was measured as a function of the filter depth (Fig. S2, SI3) (carbamazepine (low biodegradation), valsartan (intermediate biodegradation), atenolol (high biodegradation), paracetamol (high biodegradation) (Bourgin et al., 2018; Falås et al., 2016; Helbling et al., 2012)). The observed abatement of the selected compounds at a filter depth of 200 cm was in line with the expected efficiency for their biodegradability. The biological activity of the sand filter is further illustrated by the abatement of about 25% of DOC (corresponding to BDOC) during sand filtration after ozonation (Fig. S8, SI3). This abatement is caused by low molecular weight organic compounds (aldehydes, ketones, organic acids, etc.) formed during ozonation, which are degraded during the biological post-filtration (Hammes et al., 2006; Van der Kooij et al. 1989). AOC was also measured, but was below the quantification limit (10 μg/L) in all samples. Furthermore, sand samples were taken at different depths of the sand filter and protein analyses were performed to determine the bacterial density semi-quantitatively (Rudolf von Rohr et al. 2014). The bacterial density decreased from the top of the filter to about 50 cm depth, where it leveled off (Fig. S3, SI3). Even though it can be expected that sorption plays a minor role for the abatement of the MPs and OTPs, it cannot be entirely excluded. Furthermore, ion-trapping in protozoans, which are present in biologically active sand filters (Webster and Fierer 2019), could be another mode of abatement of amine-type compounds (Gulde et al., 2018). Therefore, in the following discussion, “abatement” is often used instead of “biotransformation” or “biodegradation”.

3.2.2. Parent compounds

For MPs which were abated in the sand filter, often an initially faster abatement in the first 50 cm of the sand filter column is observed, followed by a slower decrease, roughly similar to the protein density distribution in the sand filter (Fig. S3, SI3 and SI1), indicating slightly enhanced biological activities in the top part of the sand filter. From the 34 parent MPs, for which OTPs (187) were detected in high enough concentrations to be evaluated in the sandfilter, 22 (65%) were stable and 12 (35%) were abated by more than 20% in the sand filter (SI1). In general, amine-type compounds were better abated than aromatic or olefinic compounds (Fig. 6). Abatement in the sand filter for each individual MP is provided in SI1 and SI5.

3.2.3. OTPs

From the 227 OTPs that were identified, 187 OTPs from 34 parent compounds resulted in meaningful data in the sand filtration (SI1, Table S3, SI3, SI4). Three patterns could be observed for the fate of OTPs in the biological sand filtration: (i) relevant abatement, (ii) relevant formation or (iii) stability according to the classification in Section 2.4.5. It is often assumed that a partial oxidation of recalcitrant micropollutants leads to a better biodegradability of the corresponding OTPs (Lee et al., 2012). This perception is based on the efficiency of biological sand filtration for the removal of AOC and BDOC, which are formed from the oxidation of DOM (see discussion in Section 3.2.1 and Fig. S8, SI3). The current study shows that this observation does not directly translate to MPs and their OTPs. From the 187 detected OTPs, 143 (76%) were stable, 35 (19%) were abated, and 9 (5%) were formed. These results are somewhat biased because, as it has been demonstrated in the discussion of reaction mechanisms, many expected products especially from aromatic and olefinic compounds escape detection. However, based on the detected OTPs, it is clear that oxidative transformations of micropollutants does not necessarily lead to OTPs that are readily abated in biological post-treatment. This might also be caused by the fact that microorganisms were not adapted to the MPs and its OTPs because the degradation is controlled by a co-metabolic pathway (Benner et al., 2013).

From a screening of the detected OTPs, abatement can be observed for the following overarching structural features: aldehydes, carbonyls, carboxylic acids, alcohols, and amides. This comparison provides only a rough overview, because often several such functional groups can be present in OTPs and the detected functional groups are not necessarily decisive for the abatement in large molecules. Therefore, it is often unclear which functional group is responsible for the abatement. In the following discussion certain OTP types are grouped together. Aldehydes/carbonyls and carboxylic acids can be formed from the reactions of olefins and aromatic compounds and sometimes aliphatic groups with ozone and/or $^{\bullet}$OH, whereas alcohols are mostly formed from the reactions of aliphatic groups with $^{\bullet}$OH. The formation of amides is as of yet not clearly related to the classes of functional groups of this study. In a previous investigation, it has been shown by a theoretical assessment, that OTPs from olefins and aromatic compounds with the formation of the corresponding aldehydes/carbonyls and carboxylic acids are expected to have a better biodegradability than the parent compounds (Hübner et al., 2015). Furthermore, it has been demonstrated that amides are biodegradable in sewage sludge-seeded bioreactors (Helbling et al., 2010). Table S2 (SI3) provides an overview over the fate of various, newly formed functional groups of OTPs with clear structures in the biological sand filtration (aldehydes/carbonyls, aliphatic alcohols, carboxylic acids, 1°, 2° and 3° amides, *N/S*-oxides). 36% of aldehydes/carbonyls/alcohols, 29% of carboxylic acids and 27% of amides showed abatement. For the other functional groups, it was $< 20\%$ (10% for *N/S*-oxides). It has to be noted that relatively low numbers of compounds were tested in this study and therefore, these numbers just provide a rough estimate.

In the following, the 35 OTPs which show a relevant abatement in the sand filter (as differentiated in Table S3 (SI3) and SI1 from OTPs that are not abated), and for which clear structures could be proposed, will be discussed. The discussion is based on the functional groups of the OTPs.

3.2.3.1. Aldehydes, carbonyls, alcohols. Fourteen aldehyde/carbonyl/alcohol-type compounds, for which structures could be proposed and which are abated to a relevant extent in the sand filtration, are shown in Fig. 7. They include OTPs from bezafibrate, carbamazepine (2 OTPs), cetirizine, fenpropidin (3 OTPs), flecainide, prometon, propyzamide, sitagliptin (2 OTPs), tramadol and valsartan and comprise 36% of all

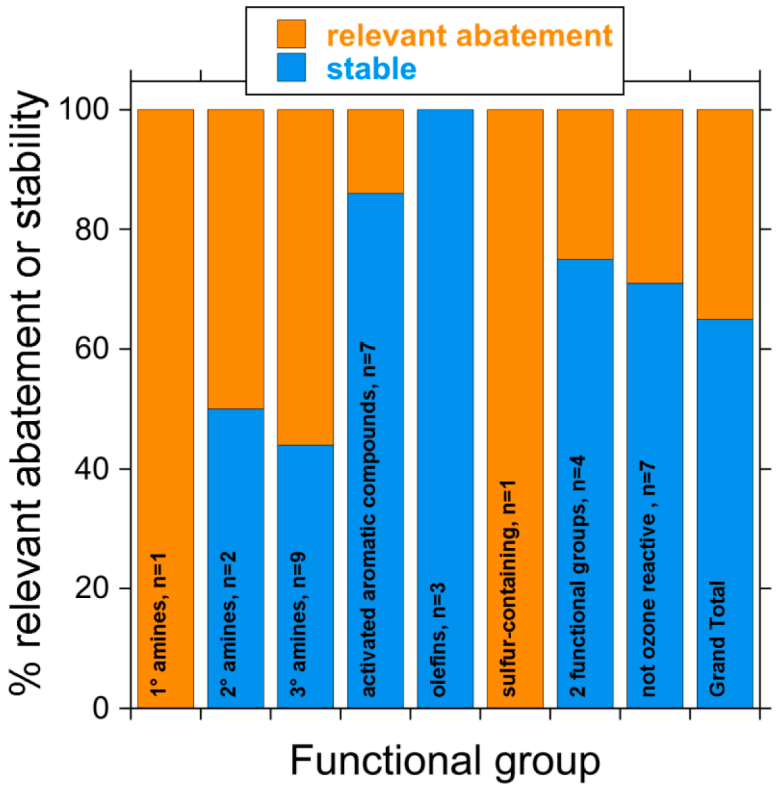

Fig. 6. Fate of selected parent MPs (34, with detected OTPs) during sand filtration, which was preconditioned for optimum biodegradation (see Section 2.2). The MPs are ordered according to their ozone-reactive functional groups. Relevant abatement is classified for relative changes $< -20\%$ (i.e., abatement $> 20\%$) (see Section 2.4.5 for a detailed description). Y-axis: % relevant abatement or stability is given relative to the total number of compounds (n) of MPs in each category.

newly formed aldehydes, carbonyls and aliphatic alcohols with proposed structures (SI1 and Table S3 (SI3)). These OTPs are related to various ozone-reactive functional groups. BZF240 is formed by ring opening of the aromatic ring of bezafibrate, with a predicted enhanced biodegradability (Hübner et al., 2015). Two products from carbamazepine are induced by an ozone attack on the olefin followed by secondary reactions (CBZ251 (BQM); CBZ179). CBZ251 has been shown previously to have an enhanced biodegradability (Hübner et al., 2014). A dealkylation of one of the tertiary amine groups in cetirizine leads to CET217 (Borowska et al., 2016) with a significant abatement in the sand filtration. Three OTPs of fenpropidin (FEN274, FEN288, FEN292), containing carbonyls or alcohols formed by $^{\bullet}$OH attack, are partially abated in the sand filter. One OTP of flecainide containing a nitro and an aldehyde group (FLE461_20.7 or FLE461_21.3, Fig. 3) is abated. Since the precursor of these products (FLE429, imine oxide) is not abated, it can be assumed that the enhancement is due to the formation of the aldehyde moiety in FLE461 (only one of the two possible products is shown in Fig. 7, see also Fig. 3). One of the products of the oxidation of prometon by $^{\bullet}$OH is PRM240 with an aldehyde on one of the isopropyl groups. This modification leads to an enhanced abatement of this OTP. An OTP as a result from the oxidation of the ethinyl group in propyzamide is formed (PYZ320) and abated in the sand filter. Two alcohol-containing secondary OTPs from sitagliptin (SIT249, SIT281) were found to be partially abated in the sand filter. The primary OTP of tramadol (TRA280) is further transformed to various other OTPs, mainly by $^{\bullet}$OH attack. One case in point is TRA328_13.1, an OTP with three additional oxygen atoms, which is caused by ring opening and addition of an alcohol group. This renders it slightly but significantly more biodegradable than tramadol or TRA312 with two additional oxygen atoms. Ion-trapping (see Section 3.2.1) cannot be the cause for the abatement of TRA328_13.1, because the tertiary amine group has been transformed to an *N*-oxide. The introduction of a carbonyl group on one of the aliphatic carbons of valsartan (VAL450) leads to a relevant abatement of this OTP.

3.2.3.2. Carboxylic acids. Carboxylic acid-type compounds for which structures could be proposed and which are relevantly abated in the sand filtration are shown in Fig. 8. These 4 OTPs are derived from bezafibrate, flecainide, propyzamide and valsartan and comprise 29% of all newly detected carboxylic acids (SI1 and Table S3 (SI3)). For bezafibrate, a formation of a carboxylic acid (with a carbonyl in α-position) has been observed as a consequence of a Criegee-type reaction on the alkoxybenzene moiety (BZF254) (Fig. 4). However, this product is not biodegradable. A related product (BZF256) has an enhanced biodegradability (it has an OH group in α-position to the carboxyl group). Its formation is not entirely clear, however, $^{\bullet}$OH reactions most likely play an important role. This example illustrates that small differences in molecular structures can have significant effects on the biodegradability of OTPs. For flecainide, an OTP with a carboxylic acid group (FLE475) seems to be even more efficiently abated than its precursor FLE461 (Fig. 7) with an aldehyde group. For the oxidation of the ethinyl group of propyzamide two carboxylic-type products have been identified (PYZ301, PYZ274). It is intriguing that PYZ301 is not biodegradable, whereas PYZ274 shows enhanced abatement. The carbonyl group in α-position to the carboxylic group in the case of PYZ301 as in BZF254 enhances the electrophilic character and may hinder the further oxidation of this product. Other carboxylic compounds are formed from the oxidation of valsartan to the corresponding benzoic acid (VAL336 in Fig. 8, VAL450 in Fig 7). Even though valsartan is also abated during sand filtration (already contains a carboxylic acid group), the OTPs VAL336 and VAL450 show an enhanced abatement.

3.2.3.3. Amides. Six amide-type compounds for which structures could be proposed and which are abated in the sand filtration are shown in Fig. 9. These OTPs are formed from bezafibrate, cephalexin, diclofenac, diuron (2 OTPs) and phenazone. Together with other well abated amides, which were discussed before as they contain also other functional groups like aldehydes (see Figs. 7 and 8), they comprise 27% of all

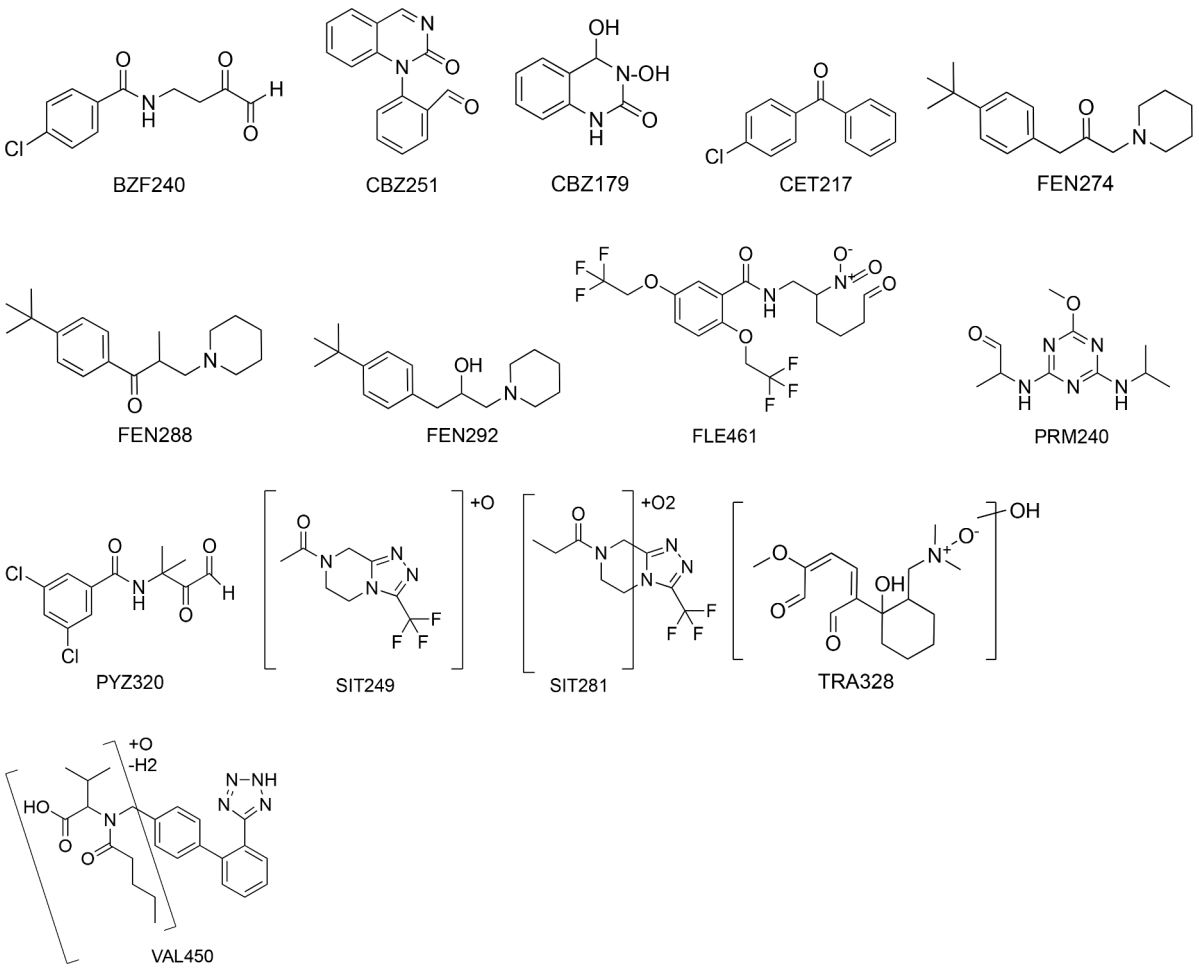

Fig. 7. Proposed structures of 14 detected alcohols/aldehyde/carbonyl-type OTPs with relevant abatement in the sand filter.

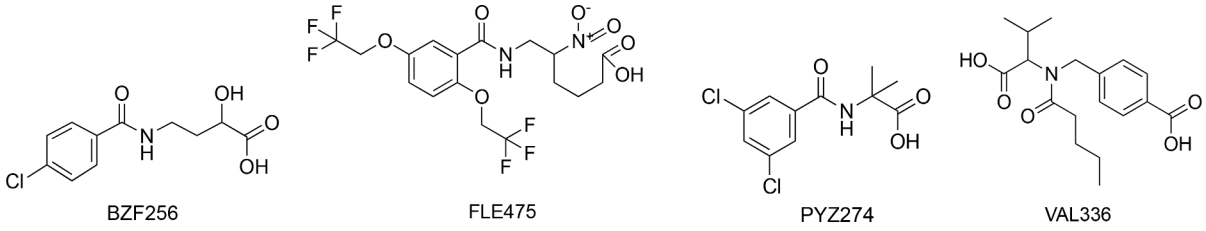

Fig. 8. Proposed structures for 4 carboxylic OTPs with relevant abatement in the sand filtration. VAL450, another carboxylic compound with additional carbonyl is already shown in Fig. 7.

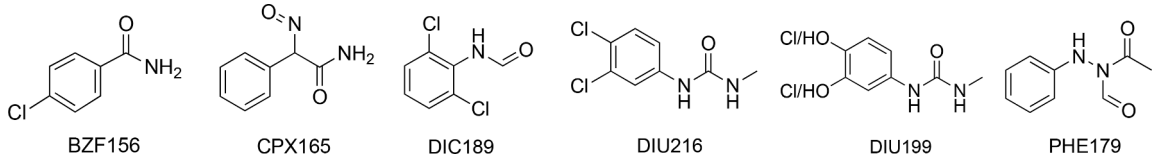

Fig. 9. Proposed structures for 6 amide-type OTPs with relevant abatement in the sand filtration.

suggested newly formed amide-type compounds (SI1 and Table S3 (SI3)). Dealkylation of the amide group of bezafibrate and cephalexin lead to the formation of primary amide structures (BZF156, CPX165). DIC189 is an amide-type secondary product of the oxidation of diclofenac with an enhanced abatement. For the formation of DIU216 from diuron, a dealkylation as for BZF156 can be assumed, for DIU199, additionally a substitution of Cl by OH has been proposed. The transformation of the tertiary amide structure in diuron to a secondary amide leads to an enhancement of the biodegradability of DIU216 as expected from a previous study (Helbling et al., 2010). The oxidation of phenazone leads to the formation of PHE179, which is significantly better abated than the parent compound.

3.2.3.4. Miscellaneous OTP structures. Three miscellaneous OTPs for

which a structure was proposed and which are abated in the sand filtration are shown in Fig. 10. These OTPs are derived from diphenhydramine, sulfamethoxazole and thiacloprid. An interesting case is the formation of DIP167 in small quantities as a secondary OTP from diphenhydramine. It is most likely formed by •OH reactions, however, a detailed formation mechanism is currently not available. SMX225, a secondary OTP of the oxidation of sulfamethoxazole, is significantly better biodegradable than its precursors. Based on the stability of SMX282 (nitro-SMX) in the sand filter, the nitrobenzene is recalcitrant and thus the secondary ring formation seems to be responsible for this observation. THI283, a sulfone-type primary OTP from thiacloprid, has a similar abatement efficiency as the parent compound, which indicates that the molecular changes might not be important for biodegradation. CLA764, the *N*-oxide of clarithromycin (not shown in Fig. 10) has a similar abatement efficiency as its parent compound, which indicates again that molecular features in the parent compound control the biodegradation (aldehydes, carbonyl groups).

Seven further OTPs were abated to a relevant extent, however the proposed structures were not clear enough to assign them to one of the discussed groups. These OTPs are FEN276, FLE301, FLE444, SIT171, SIT391, SMZ152, SMZ222 (SI1, SI2).

3.2.4. *Comparison of the abatement of parent MPs with the OTPs*

To assess the overall treatment efficiency (ozonation combined with biological sand filtration), a comparison of the abatement of parent compounds and OTPs in the sand filter was carried out.

In the following, the abatement of OTPs relative to the parent compounds is discussed for three types of cases, (i) OTPs with similar, (ii) worse or (iii) better abatement than their parent compounds (Section 2.4.5 and SI1, Table S3, SI3). For similar abatement, oxidative transformation might not have altered the biodegradable part of the structure. For worse abatement, some modifications of the biodegradable part(s) of the compound might have occurred. For better abatement, new biodegradable functional groups are formed. The OTPs with no abatement (143) or formation (9) will not be further discussed, as this would be beyond the scope of this paper. For these OTPs, the oxidative transformation does not introduce biodegradable functional groups and in the case of formation, OTPs from biological and chemical oxidation are the same and further formed from a precursor (MP or OTP).

(i) Nine OTPs with similar and relevant abatement as the corresponding parent compound

For some OTPs with similar abatement efficiency as their parent compounds, it can be assumed that the structural features, which are responsible for biodegradation, are not changed during oxidation, or some new moieties are formed which hinder biodegradation at the original site but enable new pathways of biodegradation. This was observed for 9 OTPs from four parent compounds, clarithromycin (1 OTP), fenpropidin (3 OTPs), flecainide (1 OTP) and sitagliptin (4 OTPs) (SI1).

For example, CLA764 is an *N*-oxide with a similar abatement efficiency as the parent compound CLA (SI1). Therefore, it can be hypothesized that the abatement is not related to the tertiary amine group, which is oxidized to the *N*-oxide in CLA764, but probably due to the carbonyls and alcohols in the unaltered molecule (see Section 3.2.3).

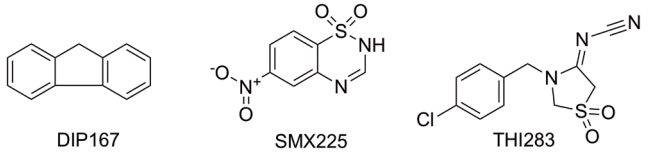

Fig. 10. Miscellaneous proposed structures for OTPs with enhanced abatement during the sand filtration.

This also excludes the hypothesis of ion-trapping for this compound (Gulde et al., 2018), which is based on the protonation of the tertiary amine group.

For fenpropidin, three OTPs fall in this category. Two OTPs (FEN274, FEN 288, Fig. 7) result from an oxidation at the aliphatic chain. The tertiary amine seems to be a critical functional group, because the FEN-*N*-oxide (FEN290) is not abated anymore. Nevertheless, if the primary *N*-oxide is oxidized to an alcohol on a side chain (FEN292, Fig. 7), an abatement is again observed. Alterations of the tert-butyl benzene functional group to a benzoquinone-type structure at the aromatic ring (e.g. FEN304, FEN320, SI1, SI2) or more significant modifications on the piperidine moiety lead to a decrease of the biodegradability. This is of importance, since it has been demonstrated that benzoquinones are potentially toxic compounds (Tentscher et al., 2021), wherefore, the persistence of these compounds in biological post-filtration is not desired.

For flecainide, which is partially biodegradable, the formation of the imine oxide (FLE429, SI1, SI2, Table S3 (SI3)) hinders a biodegradation. Also, most other detected OTPs have relevant modifications at the piperidine moiety. Therefore, it seems that an intact piperidine moiety is an important feature to enable biodegradation. Nevertheless, further oxidation to one nitro compound (FLE461, Fig. 7) enhances the biodegradability again, however, the second OTP with a nitro group and the same mass shows non-relevant abatement. It is hypothesized that the formation of a carbonyl is responsible for the degradation, however, the position of it seems decisive.

Several OTPs of sitagliptin (SIT171, SIT249, SIT281, Fig. 7) have a similar pattern in the sand filter as the parent compound. These three OTPs are significantly smaller molecules and do not contain the parent compound structure anymore. Furthermore, SIT391 also has a similar abatement efficiency as the parent compound. Overall, it is unclear why this behavior is observed for these OTPs and not for other OTPs from sitagliptin. One case in point for a none-degradable OTP is SIT436 (nitro compound). This may be problematic due to the potential toxicity of nitro compounds (Lim et al., 2019). However, it is so far unknown if nitro compounds are generally not abated in biological post-treatments.

Overall, the case of similar abatement of the parent and OTPs has been observed for only 9 OTPs (5% of all 187 OTPs) from 4 parent compounds (two tertiary amines, one secondary amine and one primary amine). The data base for these cases is relatively small, wherefore no generalizations are possible at this point.

(ii) Two OTPs with worse and relevant abatement than the corresponding parent compound

For worse abatement of the OTP, some modifications of the biodegradable part(s) of the compound might have occurred. Only two cases (1% from all 187 OTPs) with worse but relevant abatement of the OTPs were observed (FEN276 and THI283). For FEN276, derived from fenpropidin, modifications at the piperidine moiety seem to reduce the abatement efficiency as already observed for flecainide. THI283 (Fig. 10) is derived from thiacloprid with an oxidation of the thioether group. This functional group might be at least partially relevant for the biodegradability of this compound.

(iii) 24 OTPs with better and relevant abatement relative to parent compound

A biological post-treatment is often applied after ozonation to improve the biostability of the water and it would be desirable to get an abatement of OTPs at the same time. It is assumed that for a better abatement, new functional groups are introduced to the molecule or existing functional groups are modified. Overall, this case was only observed for 24 OTPs (SI1, Table S3 (SI3), Figs. 7–10), which corresponds to 13% of the detected OTPs, formed from 16 parent compounds, namely, bezafibrate (3 OTPs, BZF156, BZF240, BZF256, Figs. 7–9),

carbamazepine (2 OTPs, CBZ179, CBZ251, Fig. 7), cetirizine (1 OTP, CET217, Fig. 7), cephalexin (1 OTP, CPX165, Fig. 9), diclofenac (1 OTP, DIC189, Fig. 9), diphenhydramine (1 OTP, DIP167, Fig. 10), diuron (2 OTPs, DIU199, DIU216, Fig. 9), flecainide (3 OTPs, FLE475, Fig. 8; FLE444 and FLE301, SI1), phenazone (1 OTP, PHE179, Fig. 9), prometon (1 OTP, PRM240, Fig. 7), propyzamide (2 OTPs, PYZ320, PYZ274, Figs. 7 and 8), sulfamethoxazole (1 OTP, SMX225, Fig. 10), sulfamethazine (2 OTPs, SMZ152, SMZ222, SI1), tramadol (1 OTP, TRA328, Fig. 7), and valsartan (2 OTPs, VAL336, VAL450, Figs. 7 and 8). Most of the OTPs have been discussed in Section 3.2.3, except for the 4 OTPs FLE301, FLE444, SMZ152, and SMZ222, for which no clear structures could be derived.

From this discussion of the formation and abatement of the OTPs, it becomes evident that higher generation OTPs are often not related to the primary ozone-reactive sites in the MPs anymore. Nevertheless, a comparison of the abatement of OTPs relative to the parent compound, based on the primary ozone-reactive site, is shown in Fig. 11. In general, for amine-containing MPs, the abatement of the OTPs in the sand filter is only more efficient in rare cases, whereas for activated aromatic and olefinic moieties in the parent MP an improvement was achieved for a significant fraction of compounds (36% and 50%, respectively). Nevertheless, the general assumption that a partial oxidative transformation of micropollutants leads to better biodegradable compounds could not be confirmed in this study. From the discussion above, it is evident that the formation of aldehyde, carbonyl, alcohol, carboxylic acid and amide groups may enhance the degradation, whereas *N*-oxidation generally leads to more recalcitrant OTPs, unless another site in the molecule is responsible for its biodegradability. This also explains the relatively high proportion of worse abatement of OTPs from amine-type compounds. The two OTPs of the sulfur-containing benzisothiazolone were abated worse than their parent. MPs with several ozone reactive sites do not generally lead to OTPs with a better biodegradability than the parents, however, for this class of compounds often a similar behavior as for the parent compounds is observed. Ozone-resistant MPs react predominantly with $^{\bullet}$OH and also in this case, a limited number of OTPs (6, 18%) showed a better abatement in the sand filter than the parent compounds. This shows that $^{\bullet}$OH oxidation, and in general advanced oxidation processes, do not seem to be more efficient in terms of the formation of biodegradable OTPs than conventional ozonation.

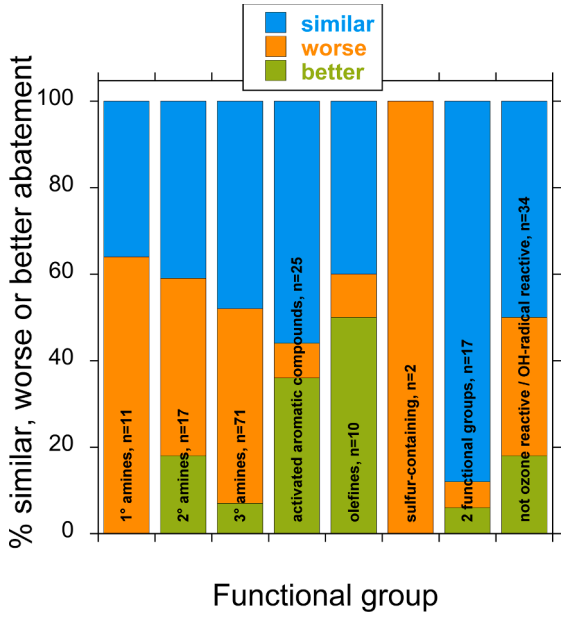

Fig. 11. Comparison of the abatement of the 34 MPs and the ensuing 187 OTPs (n in the figure) during sand filtration after ozonation. The compounds are ordered according to the main ozone-reactive functional group of the MPs, despite the fact that often higher generation products were formed, for which the initial site of ozone attack is not necessarily crucial anymore.

4. Practical implications

The combination of LC-HRMS/MS data from laboratory and pilot experiments with kinetic and mechanistic information on ozone and hydroxyl reactions can be applied to elucidate transformation product formation during ozonation with a higher plausibility than LC-HRMS/MS alone. This approach should be further developed to make significant advances in understanding the fate of micropollutants during ozonation. This information can then be further used to assess the fate of transformation products during biological post-treatment, which is applied after ozonation to abate easily biodegradable compounds formed during the reactions of ozone and hydroxyl radicals with the DOM (von Sonntag and von Gunten 2012). This has been confirmed in the current study by the observed abatement of DOC and selected micropollutants with known biodegradability in sand filtration after ozonation. The successful combination of ozonation followed by biological filtration has often been assumed to be an equally important barrier for micropollutants and their OTPs. From this study, it can be concluded that biological post-filtration is not very effective for the abatement of parent compounds and OTPs. There are some trends which may suggest that different classes of OTPs might differ in biodegradability compared to their parent MPs, however, more information would be needed to further confirm these preliminary observations. As a general rule, *N*-containing compounds might be less biodegradable after ozonation due to formation of recalcitrant N-O bonds, whereas compounds with an attack of ozone and/or $^{\bullet}$OH on the carbon structure may lead to moieties such as aldehydes/carbonyls/alcohols and carboxylic acids, which have a better chance of being biodegraded. Another class of compounds are amides, which may be formed or transformed by reactions with hydroxyl radicals, leading to biodegradable OTPs. With the analytical window applied in this study, compounds resulting from activation of aromatic moieties by phenol formation and the ensuing fast reactions with ozone, as other small and polar OTPs, might have escaped detection, which may distort the overall picture. This study demonstrates that ozonation abates micropollutants and forms a multitude of OTPs, which might persist during biological post-filtration. This process can be considered as an oxidative dilution of the target compounds leading to significantly smaller concentrations of the OTPs (von Gunten, 2018). Other studies have demonstrated that many of the biologically active compounds lose their effects and (eco)toxicological tests have shown the same (Dodd et al., 2009; Escher et al., 2009; Huber et al., 2004; Mestankova et al., 2011; Mestankova et al., 2016). However, there are also known cases, where more toxic OTPs are formed from target compounds. On case in point is the formation of *N*-nitrosodimethylamine from the bromide-catalysed reaction of dimethlysulfamide with ozone (Schmidt and Brauch 2008; von Gunten et al. 2010). Nevertheless, also due to the smaller concentrations of the OTPs, the risk of enhanced toxicity is relatively small (von Gunten 2018). A shortcoming of the currently applied analytical approach is that the mass balance is unknown and it is unclear what other OTPs are formed. To this end, detailed laboratory studies with e.g., radiolabeled compounds could yield a better quantification of the OTPs and close the deficiency in the mass balance.

5. Conclusions

Fifty-one micropollutants with various ozone-reactive sites were spiked to a pilot ozonation system and their abatement with the ensuing formation of transformation products (OTPs) was investigated. Furthermore, the fate of the micropollutants and the OTPs was investigated in a biological post-treatment with a sand filter. The following conclusions can be drawn:

- 227 OTPs from 39 parent compounds were identified after solid phase extraction by LC-HRMS/MS based on laboratory and full-scale experiments, with 187 OTPs from 34 parent compounds present in meaningful concentrations during the sand filtration.
- A rigorous kinetic and mechanistic interpretation of the chemical structures from the MS/MS data was a prerequisite to understand and explain the formation of a large number of OTPs based on ozone and hydroxyl reactions. This approach also allowed to assess the plausibility of OTPs, which were proposed in previous studies. However, also for a large number of proposed OTPs, no mechanistic interpretation could be provided, which warrants detailed studies under controlled conditions.
- 35 OTPs had a relevant abatement in the biological sand filtration, and 24 OTPs of them showed a better abatement than the corresponding parent compound. Overall, this is a low fraction (13%) of all the detected OTPs.
- It could be shown that degradable OTPs often contained aldehyde, carbonyl, carboxylic alcohol, or amide functional groups.
- It seems that many of the expected OTPs from aromatic compounds and olefins escaped detection by the applied analytical approach. This may have biased the findings of this study towards a worse outcome in terms of the fraction of biodegradable OTPs.

Declaration of Competing Interest

The authors declare that they have no known competing financial interests or personal relationships that could have appeared to influence the work reported in this paper.

Acknowledgments

Funding from the Eawag discretionary fund and the waterworks Zurich (Stadt Zürich, Wasserversorgung WVZ) are acknowledged. We thank Andreas Peter from waterworks Zurich for fruitful discussions, and the colleagues from Eawag, Andreas Scheidegger for support on the statistical evaluation and Jennifer Schollée for valuable input.

Supplementary materials

Supplementary material associated with this article can be found, in the online version, at doi:10.1016/j.watres.2021.117812.

References

Abellan, M.N., Gebhardt, W., Schroder, H.F., 2008. Detection and identification of degradation products of sulfamethoxazole by means of LC/MS and -MSn after ozone treatment. Water Sci. Technol. 58 (9), 1803–1812.
Acero, J.L., Stemmler, K., von Gunten, U., 2000. Degradation kinetics of atrazine and its degradation products with ozone and OH radicals: a predictive tool for drinking water treatment. Environ. Sci. Technol. 34, 591–597.
Azaïs, A., Mendret, J., Cazals, G., Petit, E., Brosillon, S., 2017. Ozonation as a pretreatment process for nanofiltration brines: monitoring of transformation products and toxicity evaluation. J. Hazard. Mater. 338, 381–393.
Bader, H., Hoigne, J., 1981. Determination of ozone in water by the indigo method. Water Res. 15 (4), 449–456.
Barletta, B., Bolzacchini, E., Meinardi, S., Orlandi, M., Rindone, B., 2003. The Kinetics and the mechanism of the reaction of 2-chloro-4,6-dialkylamino-1,3,5-triazines with ozone. Ozone Sci. Eng. 25 (2), 81–94.
Barron, E., Deborde, M., Rabouan, S., Mazellier, P., Legube, B., 2006. Kinetic and mechanistic investigations of progesterone reaction with ozone. Water Res. 40 (11), 2181–2189.
Beltrán, F.J., García-Araya, J.F., Álvarez, P.M., Rivas, J., 1998. Aqueous degradation of atrazine and some of its main by-products with ozone/hydrogen peroxide. J. Chem. Technol. Biotechnol. 71 (4), 345–355.
Beltran, F.J., Gonzalez, M., Rivas, J., Marin, M., 1994. Oxidation of mecoprop in water with ozone and ozone combined with hydrogen-peroxide. Ind. Eng. Chem. Res. 33 (1), 125–136.
Benitez, F.J., Real, F.J., Acero, J.L., Garcia, C., 2007. Kinetics of the transformation of phenyl-urea herbicides during ozonation of natural waters: rate constants and model predictions. Water Res. 41 (18), 4073–4084.
Benner, J., Helbling, D.E., Kohler, H.P.E., Wittebol, J., Kaiser, E., Prasse, C., Ternes, T.A., Albers, C.N., Aamand, J., Horemans, B., Springael, D., Walravens, E., Boon, N., 2013. Is biological treatment a viable alternative for micropollutant removal in drinking water treatment processes? Water Res. 47 (16), 5955–5976.
Benner, J., Salhi, E., Ternes, T., von Gunten, U., 2008. Ozonation of reverse osmosis concentrate: kinetics and efficiency of beta blocker oxidation. Water Res. 42 (12), 3003–3012.
Benner, J., Ternes, T.A., 2009. Ozonation of propranolol: formation of oxidation products. Environ. Sci. Technol. 43 (13), 5086–5093.
Bollmann, A.F., Seitz, W., Prasse, C., Lucke, T., Schulz, W., Ternes, T., 2016. Occurrence and fate of amisulpride, sulpiride, and lamotrigine in municipal wastewater treatment plants with biological treatment and ozonation. J. Hazard. Mater. 320, 204–215.
Borowska, E., Bourgin, M., Hollender, J., Kienle, C., McArdell, C.S., von Gunten, U., 2016. Oxidation of cetirizine, fexofenadine and hydrochlorothiazide during ozonation: kinetics and formation of transformation products. Water Res. 94, 350–362.
Bourgin, M., Beck, B., Boehler, M., Borowska, E., Fleiner, J., Salhi, E., Teichler, R., von Gunten, U., Siegrist, H., McArdell, C.S., 2018. Evaluation of a full-scale wastewater treatment plant upgraded with ozonation and biological post-treatments: abatement of micropollutants, formation of transformation products and oxidation by-products. Water Res. 129, 486–498.
Bourgin, M., Borowska, E., Helbing, J., Hollender, J., Kaiser, H.-.P., Kienle, C., McArdell, C.S., Simon, E., von Gunten, U., 2017. Effect of operational and water quality parameters on conventional ozonation and the advanced oxidation process O_3/H_2O_2: kinetics of micropollutant abatement, transformation product and bromate formation in a surface water. Water Res. 122, 234–245.
Broséus, R., Vincent, S., Aboulfadl, K., Daneshvar, A., Sauvé, S., Barbeau, B., Prévost, M., 2009. Ozone oxidation of pharmaceuticals, endocrine disruptors and pesticides during drinking water treatment. Water Res. 43 (18), 4707–4717.
Buffle, M.O., Schumacher, J., Meylan, S., Jekel, M., von Gunten, U., 2006a. Ozonation and advanced oxidation of wastewater: effect of O_3 dose, pH, DOM and HO.-scavengers on ozone decomposition and HO. generation. Ozone Sci. Eng. 28 (4), 247–259.
Buffle, M.O., Schumacher, J., Salhi, E., Jekel, M., von Gunten, U., 2006b. Measurement of the initial phase of ozone decomposition in water and wastewater by means of a continuous quench-flow system: application to disinfection and pharmaceutical oxidation. Water Res. 40 (9), 1884–1894.
Buffle, M.O., von Gunten, U., 2006. Phenols and amine induced HO center dot generation during the initial phase of natural water ozonation. Environ. Sci. Technol. 40 (9), 3057–3063.
Buxton, G.V., Greenstock, C.L., Helman, W.P., Ross, W.P., 1988. Critical review of rate constants for reactions of hydrated electrons, hydrogen atoms and hydroxyl radicals in aqueous solution. J. Phys. Chem. Ref. Data 17, 513–886.
Coelho, A.D., Sans, C., Agüera, A., Gómez, M.J., Esplugas, S., Dezotti, M., 2009. Effects of ozone pre-treatment on diclofenac: intermediates, biodegradability and toxicity assessment. Sci. Total Environ. 407 (11), 3572–3578.
Dantas, R.F., Canterino, M., Marotta, R., Sans, C., Esplugas, S., Andreozzi, R., 2007. Bezafibrate removal by means of ozonation: primary intermediates, kinetics, and toxicity assessment. Water Res. 41 (12), 2525–2532.
Dodd, M.C., Buffle, M.O., von Gunten, U., 2006. Oxidation of antibacterial molecules by aqueous ozone: moiety-specific reaction kinetics and application to ozone-based wastewater treatment. Environ. Sci. Technol. 40 (6), 1969–1977.
Dodd, M.C., Kohler, H.P.E., von Gunten, U., 2009. Oxidation of antibacterial compounds by ozone and hydroxyl radical: elimination of biological activity during aqueous ozonation processes. Environ. Sci. Technol. 43 (7), 2498–2504.
Dodd, M.C., Rentsch, D., Singer, H.P., Kohler, H.P.E., von Gunten, U., 2010. Transformation of beta-lactam antibacterial agents during aqueous ozonation: reaction pathways and quantitative bioassay of biologically-active oxidation products. Environ. Sci. Technol. 44 (15), 5940–5948.
Eggen, R.I.L., Hollender, J., Joss, A., Schärer, M., Stamm, C., 2014. Reducing the discharge of micropollutants in the aquatic environment: the benefits of upgrading wastewater treatment plants. Environ. Sci. Technol. 48 (14), 7683–7689.
Elovitz, M.S., von Gunten, U., 1999. Hydroxyl radical/ozone ratios during ozonation processes. I. The R_{ct} concept. Ozone Sci. Eng. 21, 239–260.
Elovitz, M.S., von Gunten, U., Kaiser, H.P., 2000. Hydroxyl radical/ozone ratios during ozonation processes. II. The effect of temperature, pH, alkalinity, and DOM properties. Ozone Sci. Eng. 22, 123–150.
Escher, B.I., Bramaz, N., Ort, C., 2009. JEM Spotlight: monitoring the treatment efficiency of a full scale ozonation on a sewage treatment plant with a mode-of-action based test battery. J. Environ. Monit. 11 (10), 1836–1846.
Falås, P., Wick, A., Castronovo, S., Habermacher, J., Ternes, T.A., Joss, A., 2016. Tracing the limits of organic micropollutant removal in biological wastewater treatment. Water Res. 95, 240–249.
Feng, J., Zheng, Z., Luan, J., Zhang, J., Wang, L., 2008. Degradation of diuron in aqueous solution by ozonation. J. Environ. Sci. Health Part B 43 (7), 576–587.
Gao, S., Zhao, Z., Xu, Y., Tian, J., Qi, H., Lin, W., Cui, F., 2014. Oxidation of sulfamethoxazole (SMX) by chlorine, ozone and permanganate-a comparative study. J. Hazard. Mater. 274, 258.
Gerrity, D., Pecson, B., Trussell, R.S., Trussell, R.R., 2013. Potable reuse treatment trains throughout the world. J. Water Supply Res. Technol. Aqua 62 (6), 321–338.
Gresch, M., Brügger, R., Meyer, A., Gujer, W., 2009. Compartmental models for continuous flow reactors derived from CFD simulations. Environ. Sci. Technol. 43 (7), 2381–2387.
Gulde, R., Anliker, S., Kohler, H.P.E., Fenner, K., 2018. Ion trapping of amines in protozoa: a novel removal mechanism for micropollutants in activated sludge. Environ. Sci. Technol. 52 (1), 52–60.

Gulde, R., Rutsch, M., Clerc, B., Schollée, J.E., von Gunten, U., McArdell, C.S., 2021. Formation of transformation products during ozonation of secondary wastewater effluent and their fate in post-treatment: from laboratory- to full-scale. Water Res. 200, 117200.
Hammes, F., Salhi, E., Koster, O., Kaiser, H.P., Egli, T., von Gunten, U., 2006. Mechanistic and kinetic evaluation of organic disinfection by-product and assimilable organic carbon (AOC) formation during the ozonation of drinking water. Water Res. 40 (12), 2275–2286.
Helbling, D.E., Hollender, J., Kohler, H.P.E., Fenner, K., 2010. Structure-based interpretation of biotransformation pathways of amide-containing compounds in sludge-seeded bioreactors. Environ. Sci. Technol. 44 (17), 6628–6635.
Helbling, D.E., Johnson, D.R., Honti, M., Fenner, K., 2012. Micropollutant biotransformation kinetics associate with WWTP process parameters and microbial community characteristics. Environ. Sci. Technol. 46 (19), 10579–10588.
Hermes, N., Jewell, K.S., Falås, P., Lutze, H.V., Wick, A., Ternes, T.A., 2020. Ozonation of sitagliptin: removal kinetics and elucidation of oxidative transformation products. Environ. Sci. Technol. 54 (17), 10588–10598.
Hijnen, W.A.M., Voogt, R., Veenendaal, H., van der Jagt, H., Van der Kooij, D, 1995. Bromate reduction by denitrifying bacteria. Appl. Environ. Microbiol. 61, 239–244.
Hoigné, J., Bader, H., 1975. Ozonation of water: role of hydroxyl radicals as oxidizing intermediates. Science 190, 782–784 (Journal Article).
Hoigné, J., Bader, H., 1983a. Rate constants of reactions of ozone with organic and inorganic compounds in water. I. Non-dissociating organic compounds. Water Res. 17, 173–183.
Hoigné, J., Bader, H., 1983b. Rate constants of reactions of ozone with organic and inorganic-compounds in water 2. Dissociating organic-compounds. Water Res. 17 (2), 185–194.
Hollender, J., Zimmermann, S.G., Koepke, S., Krauss, M., McArdell, C.S., Ort, C., Singer, H., von Gunten, U., Siegrist, H., 2009. Elimination of organic micropollutants in a municipal wastewater treatment plant upgraded with a full-scale post-ozonation followed by sand filtration. Environ. Sci. Technol. 43 (20), 7862–7869.
Huber, M.M., Canonica, S., Park, G.Y., Von Gunten, U., 2003. Oxidation of pharmaceuticals during ozonation and advanced oxidation processes. Environ. Sci. Technol. 37 (5), 1016–1024.
Huber, M.M., Ternes, T.A., von Gunten, U., 2004. Removal of estrogenic activity and formation of oxidation products during ozonation of 17 alpha-ethinylestradiol. Environ. Sci. Technol. 38 (19), 5177–5186.
Hübner, U., Seiwert, B., Reemtsma, T., Jekel, M., 2014. Ozonation products of carbamazepine and their removal from secondary effluents by soil aquifer treatment - Indications from column experiments. Water Res. 49 (0), 34–43.
Hübner, U., von Gunten, U., Jekel, M., 2015. Evaluation of the persistence of transformation products from ozonation of trace organic compounds - a critical review. Water Res. 68, 150–170.
Kaiser, H.P., Köster, O., Gresch, M., Périsset, P.M.J., Jäggi, P., Salhi, E., von Gunten, U., 2013. Process control for ozonation systems: a novel real-time approach. Ozone Sci. Eng. 35 (3), 168–185.
Keen, O.S., Ferrer, I., Michael Thurman, E., Linden, K.G., 2014. Degradation pathways of lamotrigine under advanced treatment by direct UV photolysis, hydroxyl radicals, and ozone. Chemosphere 117, 316–323.
Keen, O.S., Linden, K.G., 2013. Re-engineering an artificial sweetener: transforming sucralose residuals in water via advanced oxidation. Environ. Sci. Technol. 47 (13), 6799–6805.
Kharel, S., Stapf, M., Miehe, U., Ekblad, M., Cimbritz, M., Falås, P., Nilsson, J., Sehlén, R., Bregendahl, J., Bester, K., 2021. Removal of pharmaceutical metabolites in wastewater ozonation including their fate in different post-treatments. Sci. Total Environ. 759, 143989.
Kråkström, M., Saeid, S., Tolvanen, P., Kumar, N., Salmi, T., Kronberg, L., Eklund, P., 2020. Ozonation of carbamazepine and its main transformation products: product determination and reaction mechanisms. Environ. Sci. Pollut. Res. 27 (18), 23258–23269.
Lajeunesse, A., Blais, M., Barbeau, B., Sauve, S., Gagnon, C., 2013. Ozone oxidation of antidepressants in wastewater -treatment evaluation and characterization of new by-products by LC-QToFMS. Chem. Cent. J. 7 (1), 15.
Lange, F., Cornelissen, S., Kubac, D., Sein, M.M., von Sonntag, J., Hannich, C.B., Golloch, A., Heipieper, H.J., Moder, M., von Sonntag, C., 2006. Degradation of macrolide antibiotics by ozone: a mechanistic case study with clarithromycin. Chemosphere 65 (1), 17–23.
Lee, C.O., Howe, K.J., Thomson, B.M., 2012. Ozone and biofiltration as an alternative to reverse osmosis for removing PPCPs and micropollutants from treated wastewater. Water Res. 46 (4), 1005–1014.
Lee, M., Zimmermann-Steffens, S.G., Arey, J.S., Fenner, K., von Gunten, U., 2015. Development of prediction models for the reactivity of organic compounds with ozone in aqueous solution by quantum chemical calculations: the role of delocalized and localized molecular orbitals. Environ. Sci. Technol. 49 (16), 9925–9935.
Lee, Y., Kovalova, L., McArdell, C.S., von Gunten, U., 2014. Prediction of micropollutant elimination during ozonation of a hospital wastewater effluent. Water Res. 64 (0), 134–148.
Lee, Y., Lee, C., Yoon, J., 2004. Kinetics and mechanisms of DMSO (dimethylsulfoxide) degradation by UV/H_2O_2 process. Water Res. 38 (10), 2579–2588.
Lee, Y., von Gunten, U., 2012. Quantitative structure-Activity relationships (QSARs) for the transformation of organic micropollutants during oxidative water treatment. Water Res. 46 (19), 6177–6195.
Lee, Y., von Gunten, U., 2016. Advances in predicting organic contaminant abatement during ozonation of municipal wastewater effluent: reaction kinetics, transformation products, and changes of biological effects. Environ. Sci. Water Res. Technol. 2 (3), 421–442.
Lester, Y., Mamane, H., Zucker, I., Avisar, D, 2013. Treating wastewater from a pharmaceutical formulation facility by biological process and ozone. Water Res. 47 (13), 4349–4356.
Li, A., Chen, Z., Wu, Q.Y., Huang, M.H., Liu, Z.Y., Chen, P., Mei, L.C., Hu, H.Y., 2016. Study on the removal of benzisothiazolinone biocide and its toxicity: the effectiveness of ozonation. Chem. Eng. J. 300, 376–383.
Lim, S., Lee, W., Na, S., Shin, J., Lee, Y., 2016. N-nitrosodimethylamine (NDMA) formation during ozonation of N,N-dimethylhydrazine compounds: reaction kinetics, mechanisms, and implications for NDMA formation control. Water Res. 105, 119–128.
Lim, S., McArdell, C.S., von Gunten, U., 2019. Reactions of aliphatic amines with ozone: kinetics and mechanisms. Water Res. 157, 514–528.
Marron, E.L., Prasse, C., Buren, J.V., Sedlak, D.L., 2020. Formation and fate of carbonyls in potable water reuse systems. Environ. Sci. Technol. 54 (17), 10895–10903.
Martín de Vidales, M.J., Robles-Molina, J., Domínguez-Romero, J.C., Cañizares, P., Sáez, C., Molina-Díaz, A., Rodrigo, M.A., 2012. Removal of sulfamethoxazole from waters and wastewaters by conductive-diamond electrochemical oxidation. J. Chem. Technol. Biotechnol. 87 (10), 1441–1449.
McDowell, D.C., Huber, M.M., Wagner, M., von Gunten, U., Ternes, T.A., 2005. Ozonation of carbamazepine in drinking water: identification and kinetic study of major oxidation products. Environ. Sci. Technol. 39 (20), 8014–8022.
Merel, S., Lege, S., Yanez Heras, J.E., Zwiener, C., 2017. Assessment of N-Oxide formation during wastewater ozonation. Environ. Sci. Technol. 51 (1), 410–417.
Mestankova, H., Escher, B., Schirmer, K., von Gunten, U., Canonica, S., 2011. Evolution of algal toxicity during (photo)oxidative degradation of diuron. Aquat. Toxicol. 101 (2), 466–473.
Mestankova, H., Parker, A.M., Bramaz, N., Canonica, S., Schirmer, K., von Gunten, U., Linden, K.G., 2016. Transformation of contaminant candidate list (CCL3) compounds during ozonation and advanced oxidation processes in drinking water: assessment of biological effects. Water Res. 93, 110–120.
Mestankova, H., Schirmer, K., Escher, B.I., von Gunten, U., Canonica, S., 2012. Removal of the antiviral agent oseltamivir and its biological activity by oxidative processes. Environ. Pollut. 161, 30–35.
Munoz, F., von Sonntag, C., 2000. Determination of fast ozone reactions in aqueous solution by competition kinetics. J. Chem. Soc., Dalton Trans. 2, 661–664.
Mvula, E., von Sonntag, C., 2003. Ozonolysis of phenols in aqueous solution. Org. Biomol. Chem. 1 (10), 1749–1756.
Olivieri, A.W., Crook, J., Anderson, M.A., Bull, R.J., Drewes, J.E., Haas, C., Jakubowski, W., McCarty, P.L., Nelson, K.L., Rose, J.B., Sedlak, D.L., Wade, T.J., 2016. Evaluation of the Feasibility of Developing Uniform Water Recycling Criteria For Direct Potable Reuse. National Water Research Institute, Fountain Valley.
Pan, X.M., Schuchmann, M.N., von Sonntag, C., 1993. Oxidation of benzene by the OH radical - a product and pulse-radiolysis study in oxygenated aqueous solutions. J. Chem. Soc. Perkin Trans. 2, 289–297.
Prasse, C., Stalter, D., Schulte-Oehlmann, U., Oehlmann, J., Ternes, T.A., 2015. Spoilt for choice: a critical review on the chemical and biological assessment of current wastewater treatment technologies. Water Res. 87, 237–270.
Pryor, W.A., Giamalva, D.H., Church, D.F., 1984. Kinetics of ozonation. 2. Amino acids and model compounds in water and comparisons to rates in nonpolar solvents. J. Am. Chem. Soc. 106, 7094–7100.
Qiang, Z., Adams, C., Surampalli, R., 2004. Determination of ozonation rate constants for lincomycin and spectinomycin. Ozone Sci. Eng. 26 (6), 525–537.
Ramseier, M.K., von Gunten, U., 2009. Mechanisms of phenol ozonation-kinetics of formation of primary and secondary reaction products. Ozone Sci. Eng. 31 (3), 201–215.
Reisz, E., Fischbacher, A., Naumov, S., von Sonntag, C., Schmidt, T.C., 2014. Hydride Transfer: a dominating reaction of ozone with tertiary butanol and formate ion in aqueous solution. Ozone Sci. Eng. 36 (6), 532–539.
Reungoat, J., Escher, B.I., Macova, M., Argaud, F.X., Gernjak, W., Keller, J., 2012. Ozonation and biological activated carbon filtration of wastewater treatment plant effluents. Water Res. 46 (3), 863–872.
Reungoat, J., Macova, M., Escher, B.I., Carswell, S., Mueller, J.F., Keller, J., 2010. Removal of micropollutants and reduction of biological activity in a full scale reclamation plant using ozonation and activated carbon filtration. Water Res. 44 (2), 625–637.
Rivas, F.J., Solís, R.R., Beltrán, F.J., Gimeno, O., 2019. Sunlight driven photolytic ozonation as an advanced oxidation process in the oxidation of bezafibrate, cotinine and iopamidol. Water Res. 151, 226–242.
Rosal, R., RodrÌguez, A., PerdigÛn-MelÛn, J.A., Petre, A., GarcÌa-Calvo, E., GÛmez, M.J., Ag¸era, A., Fern•ndez-Alba, A.R, 2009. Degradation of caffeine and identification of the transformation products generated by ozonation. Chemosphere 74 (6), 825–831.
Rosario-Ortiz, F., Rose, J., Speight, V., von Gunten, U., Schnoor, J., 2016. How do you like your tap water? Science 351 (6276), 912–914.
Rudolf von Rohr, M., Hering, J.G., Kohler, H.P.E., von Gunten, U., 2014. Column studies to assess the effects of climate variables on redox processes during riverbank filtration. Water Res. 61 (0), 263–275.
Salhi, E., von Gunten, U., 1999. Simultaneous determination of bromide, bromate and nitrite in low ug/L levels by ion chromatography without sample pretreatment. Water Res. 33, 3239–3244.
Scheurer, M., Godejohann, M., Wick, A., Happel, O., Ternes, T., Brauch, H.J., Ruck, W., Lange, F., 2012. Structural elucidation of main ozonation products of the artificial sweeteners cyclamate and acesulfame. Environ. Sci. Pollut. Res. 19 (4), 1107–1118.
Schmidt, C.K., Brauch, H.J., 2008. N,N-dimethylsulfamide as precursor for N-nitrosodimethylamine (NDMA) formation upon ozonation and its fate during drinking water treatment. Environ. Sci. Technol. 42 (17), 6340–6346.

Schymanski, E.L., Jeon, J., Gulde, R., Fenner, K., Ruff, M., Singer, H.P., Hollender, J., 2014. Identifying small molecules via high resolution mass spectrometry: communicating confidence. Environ. Sci. Technol. 48 (4), 2097–2098.
Sein, M.M., Zedda, M., Tuerk, J., Schmidt, T.C., Golloch, A., von Sonntag, C., 2008. Oxidation of diclofenac with ozone in aqueous solution. Environ. Sci. Technol. 42 (17), 6656–6662.
Shah, A.D., Liu, Z.-.Q., Salhi, E., Hofer, T., Werschkun, B., von Gunten, U., 2015. Formation of disinfection by-products during ballast water treatment with ozone, chlorine, and peracetic acid: influence of water quality parameters. Environ. Sci. Water Res. Technol. 1 (4), 465–480.
Shi, J.L., McCurry, D.L., 2020. Transformation of N-methylamine drugs during wastewater ozonation: formation of nitromethane, an efficient precursor to halonitromethanes. Environ. Sci. Technol. 54 (4), 2182–2191.
Solís, R.R., Rivas, F.J., Martínez-Piernas, A., Agüera, A., 2016. Ozonation, photocatalysis and photocatalytic ozonation of diuron. Intermediates identification. Chem. Eng. J. 292, 72–81.
Staehelin, J., Bühler, R.E., Hoigné, J., 1984. Ozone Decomposition in water studied by pulse radiolysis 2. OH and HO_4 as chain intermediates. J. Phys. Chem. 88, 5999–6004.
Stalter, D., Magdeburg, A., Weil, M., Knacker, T., Oehlmann, J., 2010. Toxication or detoxication? *In vivo* toxicity assessment of ozonation as advanced wastewater treatment with the rainbow trout. Water Res. 44 (2), 439–448.
Sui, Q., Gebhardt, W., Schröder, H.F., Zhao, W., Lu, S., Yu, G., 2017. Identification of new oxidation products of bezafibrate for better understanding of its toxicity evolution and oxidation mechanisms during ozonation. Environ. Sci. Technol. 51 (4), 2262–2270.
Tauber, A., von Sonntag, C., 2000. Products and kinetics of the OH-radical-induced dealkylation of atrazine. Acta Hydrochim. Et Hydrobiol. 28 (1), 15–23.
Tekle-Röttering, A., Jewell, K.S., Reisz, E., Lutze, H.V., Ternes, T.A., Schmidt, W., Schmidt, T.C., 2016a. Ozonation of piperidine, piperazine and morpholine: kinetics, stoichiometry, product formation and mechanistic considerations. Water Res. 88, 960–971.
Tekle-Röttering, A., Lim, S., Reisz, E., Lutze, H.V., Abdighahroudi, M.S., Willach, S., Schmidt, W., Tentscher, P.R., Rentsch, D., McArdell, C.S., Schmidt, T.C., von Gunten, U., 2020. Reactions of pyrrole, imidazole, and pyrazole with ozone: kinetics and mechanisms. Environ. Sci. Water Res. Technol. 6 (4), 976–992.
Tekle-Röttering, A., Reisz, E., Jewell, K.S., Lutze, H.V., Ternes, T.A., Schmidt, W., Schmidt, T.C., 2016b. Ozonation of pyridine and other N-heterocyclic aromatic compounds: kinetics, stoichiometry, identification of products and elucidation of pathways. Water Res. 102, 582–593.
Tentscher, P.R., Bourgin, M., von Gunten, U., 2018. Ozonation of para-substituted phenolic compounds yields p-benzoquinones, other cyclic α,β-unsaturated ketones, and substituted catechols. Environ. Sci. Technol. 52 (8), 4763–4773.
Tentscher, P.R., Escher, B.I., Schlichting, R., König, M., Bramaz, N., Schirmer, K., von Gunten, U., 2021. Toxic effects of substituted p-benzoquinones and hydroquinones in in vitro bioassays are altered by reactions with the cell assay medium. Water Res. 202, 117415.
Ternes, T.A., Stuber, J., Herrmann, N., McDowell, D., Ried, A., Kampmann, M., Teiser, B., 2003. Ozonation: a tool for removal of pharmaceuticals, contrast media and musk fragrances from wastewater? Water Res. 37 (8), 1976–1982.
Van der Kooij, D., Hijnen, W.A.M., Kruithof, J., 1989. The effects of ozonation, biological filtration and the distribution on the concentration of easily assimilable organic carbon (AOC) in drinking water. Ozone Sci. Eng. 11, 297.
von Gunten, U., 2018. Oxidation processes in water treatment: are we on track? Environ. Sci. Technol. 52 (9), 5062–5075.
von Gunten, U., Hoigné, J., 1994. Bromate formation during ozonation of bromide-containing waters: interaction of ozone and hydroxyl radical reactions. Environ. Sci. Technol. 28, 1234–1242.
von Gunten, U., Salhi, E., Schmidt, C.K., Arnold, W.A., 2010. Kinetics and mechanisms of *N*-nitrosodimethylamine formation upon ozonation of *N,N*-dimethylsulfamide-containing waters: bromide catalysis. Environ. Sci. Technol. 44 (15), 5762–5768.
von Sonntag, C., Schuchmann, H.P., Alfassi, Z.B., 1997. Peroxyl Radicals. John Wiley & Sons Ltd (ed), pp. 173-234.
von Sonntag, C., von Gunten, U., 2012. Chemistry of Ozone in Water and Wastewater treatment. From basic Principles to Applications. IWA, London.
Webster, T.M., Fierer, N., 2019. Microbial dynamics of biosand filters and contributions of the microbial food web to effective treatment of wastewater-impacted water sources. Appl. Environ. Microbiol. 85 (17) e01142-01119.
WHO, 2017. Guidelines For Drinking Water Quality, 4th ed. World Health Organization, Geneva.
Willach, S., Lutze, H.V., Eckey, K., Löppenberg, K., Lüling, M., Terhalle, J., Wolbert, J.-.B., Jochmann, M.A., Karst, U., Schmidt, T.C., 2017. Degradation of sulfamethoxazole using ozone and chlorine dioxide - Compound-specific stable isotope analysis, transformation product analysis and mechanistic aspects. Water Res. 122, 280–289 (Supplement C).
Zhang, S., Zhao, Y., Yu, G., Wang, B., Huang, J., Deng, S., 2015. Dual roles of hydroxyl radicals and effects of competition on ozonation kinetics of two phenazone-type pollutants. Emerg. Contam. 1 (1), 2–7.
Zimmermann, S.G., Schmukat, A., Schulz, M., Benner, J., von Gunten, U., Ternes, T.A., 2012. Kinetic and mechanistic investigations of the oxidation of tramadol by ferrate and ozone. Environ. Sci. Technol. 46 (2), 876–884.
Zimmermann, S.G., Wittenwiler, M., Hollender, J., Krauss, M., Ort, C., Siegrist, H., von Gunten, U., 2011. Kinetic assessment and modeling of an ozonation step for full-scale municipal wastewater treatment: micropollutant oxidation, by-product formation and disinfection. Water Res. 45 (2), 605–617.
Zucker, I., Mamane, H., Riani, A., Gozlan, I., Avisar, D, 2018. Formation and degradation of N-oxide venlafaxine during ozonation and biological post-treatment. Sci. Total Environ. 619-620, 578–586.